



HAL
open science

Chemistry and Photochemistry of Pyruvic Acid at the Air-Water Interface

Keaten Kappes, Alexandra Deal, Malte Jespersen, Sandra Blair,
Jean-Francois Doussin, Mathieu Cazaunau, Edouard Pangui, Brianna Hopper,
Matthew Johnson, Veronica Vaida

► **To cite this version:**

Keaten Kappes, Alexandra Deal, Malte Jespersen, Sandra Blair, Jean-Francois Doussin, et al.. Chemistry and Photochemistry of Pyruvic Acid at the Air-Water Interface. *Journal of Physical Chemistry A*, 2021, 125 (4), pp.1036-1049. 10.1021/acs.jpca.0c09096 . hal-03416298

HAL Id: hal-03416298

<https://cnrs.hal.science/hal-03416298>

Submitted on 5 Nov 2021

HAL is a multi-disciplinary open access archive for the deposit and dissemination of scientific research documents, whether they are published or not. The documents may come from teaching and research institutions in France or abroad, or from public or private research centers.

L'archive ouverte pluridisciplinaire **HAL**, est destinée au dépôt et à la diffusion de documents scientifiques de niveau recherche, publiés ou non, émanant des établissements d'enseignement et de recherche français ou étrangers, des laboratoires publics ou privés.

This document is confidential and is proprietary to the American Chemical Society and its authors. Do not copy or disclose without written permission. If you have received this item in error, notify the sender and delete all copies.

Chemistry and Photochemistry of Pyruvic Acid at the Air-Water Interface

Journal:	<i>The Journal of Physical Chemistry</i>
Manuscript ID	jp-2020-09096c.R2
Manuscript Type:	Special Issue Article
Date Submitted by the Author:	n/a
Complete List of Authors:	Kappes, Keaten; University of Colorado at Boulder, Chemistry Deal, Alexandra; University of Colorado at Boulder, Chemistry Jespersen, Malte ; University of Copenhagen, Department of Chemistry Blair, Sandra; University of Colorado at Boulder, Doussin, Jean-Francois; University of Paris East, LISA Cazaunau, Mathieu; Laboratoire Interuniversitaire des Systèmes Atmosphériques (LISA), Université Paris-Est Créteil Val de Marne(UPEC) Pangui, Edouard; University Paris Est Creteil, Hopper, Brianna; University of Colorado Boulder, Chemistry Johnson, Matthew; University of Copenhagen, Department of Chemistry Vaida, Veronica; University of Colorado Boulder, Chemistry

SCHOLARONE™
Manuscripts

1
2
3
4
5
6
7
8
9
10
11
12
13
14
15
16
17
18
19
20
21
22
23
24
25
26
27
28
29
30
31
32
33
34
35
36
37
38
39
40
41
42
43
44
45
46
47
48
49
50
51
52
53
54
55
56
57
58
59
60

Chemistry and Photochemistry of Pyruvic Acid at the Air-Water Interface

*Keaten J. Kappes[†], Alexandra M. Deal[†], Malte F. Jespersen[‡], Sandra L. Blair[†], Jean-Francois
Doussin[§], Mathieu Cazaunau[§], Edouard Pangui[§], Brianna N. Hopper[†], Matthew S. Johnson[‡],
Veronica Vaida^{†*}*

* Corresponding Author email: vaida@colorado.edu

[†] Department of Chemistry and Cooperative Institute for Research in Environmental Sciences,
University of Colorado Boulder, Boulder, Colorado 80309, United States

[‡] Department of Chemistry, University of Copenhagen, Universitetsparken 5, DK-2100
Copenhagen Ø, Denmark

[§] Laboratoire Interuniversitaire des Systemes Atmospheriques (LISA), UMR CNRS 7583,
Institut Pierre Simon Laplace (IPSL), Université Paris-Est Creteil (UPEC) et Université Paris
(UP), 94010 Creteil, France

Abstract

Interfacial regions are a unique chemical reaction environment that can promote chemistry not found elsewhere. The air-water interface is ubiquitous in the natural environment in the form of ocean surfaces and aqueous atmospheric aerosols. Here we investigate the chemistry and photochemistry of pyruvic acid (PA), a common environmental species, at the air-water interface and compare it to its aqueous bulk chemistry using two different experimental setups: 1) a Langmuir-Blodgett trough, which models natural water surfaces and provides a direct comparison between the two reaction environments and 2) an atmospheric simulation chamber (CESAM) to monitor the chemical processing of nebulized aqueous PA droplets. The results show that surface chemistry leads to substantial oligomer formation. The sequence begins with the dehydration of lactic acid (LA), formed at the surface, with itself and with pyruvic acid, $LA + LA - H_2O$ and $LA + PA - H_2O$ are prominent among the products, in addition to a series of higher molecular weight oligomers of mixed units of PA and LA. In addition, we see zymonic acid at the surface. Actinic radiation enhances the production of the oligomers and produces additional surface active molecules known from the established aqueous photochemical mechanisms. The presence and formation of complex organic molecules at the air-water interface from a simple precursor, like PA, in the natural environment is relevant to contemporary atmospheric science and is important in the context of prebiotic chemistry where abiotic production of complex molecules is necessary for abiogenesis.

Introduction

Heterogeneous chemistry occurring in aerosols, clouds, fogs, and at the ocean surface is significant in the natural environment, affecting atmospheric chemistry and climate.¹⁻⁹ In the environment, heterogeneous processing occurs at surfaces and interfaces which provide unique

1
2
3 reaction conditions where chemistry proceeds by different mechanisms than in bulk phases.^{2-3, 5,}
4
5 8-18 These unique reaction conditions could be caused by gradients in concentrations, molecular
6
7 alignment, water activity and electrical fields at a surface, perturbations to chromophores, or
8
9 ionization states that differ from bulk solution.^{8, 19-21} Globally distributed aerosols and cloud
10
11 droplets have an enormous collective surface area.^{3, 11, 22} In fact, the total surface area of aerosols
12
13 is greater than the combined surface area of all Earth's bodies of water²³ and provides salient
14
15 reaction locations in environmental chemistry.^{3, 8-9, 24-26}
16
17
18

19 Aqueous aerosols have additionally been proposed to be effective prebiotic chemical reactors.^{11,}
20
21 13-14, 27-31 Formed via wind action at the ocean surface, marine aerosols contain organic material
22
23 found on the ocean surface.^{3, 11, 27, 32} The ocean surface collects and concentrates hydrophobic
24
25 species from the bulk ocean, the atmosphere, hydrothermal vents, and extraterrestrial infall and
26
27 then emits these species as sea spray aerosol.^{11, 27, 31} Marine aerosols, therefore, likely contained
28
29 the monomeric precursors for complex biomolecules that are thought to have been extant on
30
31 prebiotic Earth.^{27, 30} Specifically, the surface of an aerosol provides an environment which is water-
32
33 restricted and in which organics from the sea-surface micro layer (SML) self-assemble into a
34
35 monolayer where the molecules are aligned and concentrated.^{3, 8, 11, 27, 30, 33}
36
37
38
39

40 The realization that water surfaces can host unique environmental chemistry motivated
41
42 investigations of organic molecules at the air-water interface.^{3, 8, 24-25, 34-42} Surface-specific methods
43
44 were needed for these studies. For example, nonlinear spectroscopy provided useful information
45
46 regarding the structure, ion partitioning, and orientation of surfactants at the air-water interface,⁴³⁻
47
48 ⁵⁴ while Time-of-Flight Secondary Ion Mass Spectrometry (ToF-SIMS) offered relatively
49
50 straightforward molecular identification at the interfacial region.^{37, 55-59} However, with a few
51
52 notable exceptions of dark^{12, 56, 60} and photochemical^{17-18, 37, 57, 61-66} reactions, relatively little is
53
54
55
56
57
58
59
60

1
2
3 known about the chemistry and photochemistry of organic species on water and the partitioning of
4 products from the bulk to the surface of water.
5
6

7
8 In this study we investigate the chemistry of pyruvic acid (PA) at the surface of water as it
9 provides an example of a relatively small surfactant molecule with multiple conformers and
10 environment specific reactivity. PA is naturally found in the gas phase, atmospheric aerosols, polar
11 ice, and precipitation from both direct emission and isoprene oxidation.⁶⁷⁻⁷⁰ Its multiphase
12 environmental processing is, therefore, of interest in many facets of atmospheric research,
13 especially as it can alter the chemical and optical properties of atmospheric particles.^{3, 17, 27} The
14 deprotonated form of pyruvic acid, pyruvate, has a long history in biology including a central role
15 in both aerobic and anaerobic metabolism on modern Earth where it is oxidized to acetyl CoA or
16 reduced to lactate, respectively. PA may have also contributed to abiogenesis as part of a
17 rudimentary metabolism⁷¹⁻⁷⁶ as it likely would have been available on prebiotic Earth either
18 through abiotic synthesis⁷¹ or delivery by meteorites⁷². Griffith et al.⁷³ further pointed to the
19 prebiotic relevance of PA demonstrating its photochemical production of the modern metabolites
20 acetoin and lactic acid as well as molecules larger and more complex than PA.
21
22
23
24
25
26
27
28
29
30
31
32
33
34
35
36

37
38 Previous studies of the gas- and aqueous-phase chemistry of PA are the foundation of this work.
39 The chemistry of PA in the gas-phase has been extensively studied⁷⁷⁻⁸⁶ and, unlike most organics,
40 the rate of oxidation of PA by $\cdot\text{OH}$ or HO_2 is slow and, therefore, its atmospheric fate is determined
41 by the direct absorption of sunlight by PA and the subsequent photochemical reactions^{81, 87}. Gas-
42 phase photolysis of PA occurs on the singlet manifold, mainly producing CO_2 and
43 methylhydroxycarbene, which isomerizes to acetaldehyde.^{85-86, 88-89} This process occurs with a
44 quantum yield of 1 for low buffer gas pressures.^{77, 82, 85-86}
45
46
47
48
49
50
51
52
53
54
55
56
57
58
59
60

1
2
3 The mechanisms of aqueous photochemistry of PA proceed through a different pathway than
4 the gas-phase photolysis.⁸⁹⁻⁹⁹ Briefly, diffuse UV radiation can excite a PA molecule to its S_1 state
5 which then undergoes intersystem crossing to the T_1 state and generates organic radicals, finally
6 resulting in several complex oligomers depending on the specific reaction conditions. The effects
7 of concentration, pH, and O_2 on the reaction mechanism, product yields, and array of products in
8 aqueous phase have all been described.^{37, 57, 63, 73, 90-93, 96-103} Interpreted using the gas- and aqueous-
9 phase photochemistry of pyruvic acid, the multiphase chemistry of PA has been studied,
10 highlighting the formation of oligomers and, consequently, building chemical complexity with
11 sunlight.¹⁷ Results from the study of multiphase chemistry of pyruvic acid indicate that the air-
12 water interface played a significant role in promoting chemistry not possible in either gas or bulk
13 aqueous phase.¹⁷ Another investigation reached a similar conclusion by modifying their sample
14 preparation methods to simulate the difference between bulk and interfacial photochemistry and
15 observed higher molecular weight compounds to be enhanced at the surface relative to the bulk.³⁷

16
17
18
19
20
21
22
23
24
25
26
27
28
29
30
31
32
33 In this study, we examine the chemistry and photochemistry of pyruvic acid at the air-water
34 interface. We use a combination of Langmuir-Blodgett troughs and simulation chamber studies to
35 model environmental air-water interfaces, including the surface of nebulized microdroplets. These
36 studies aim to elucidate the role the water surface plays in the multiphase chemistry of pyruvic
37 acid. Chemical and photochemical experiments provide key distinctions between reactions at the
38 air-water interface and the bulk aqueous solutions. Comparison of the results from chemistry
39 conducted on a flat air-water interface (Langmuir-Blodgett trough) with results from nebulized
40 droplets in an environmental simulation chamber (CESAM)^{17, 79, 104} highlight the chemistry
41 specific to the air-water interface. Finally, we comment on the importance of pyruvic acid's unique
42 chemistry at the air-water interface to modern and prebiotic environmental chemistry.

43 44 45 46 47 48 49 50 51 52 53 54 55 56 **Methods**

1
2
3 *Sample Preparation:*
4

5 Pyruvic acid (Sigma Aldrich, 98%) was vacuum distilled ($P < 1$ mbar) with stirring and heating
6 ($T < 70$ °C) to remove impurities. Nuclear magnetic resonance spectroscopy (NMR) was used to
7 demonstrate the purity of pyruvic acid (see Supporting Information for details and Figure S1). The
8 purified pyruvic acid was stored at 2 °C in the dark and used within one month of distillation to
9 minimize dark aging processes that could generate oligomeric species.^{17, 92, 99, 105} Aqueous
10 solutions of pyruvic acid were prepared in 18.2 MΩ (3 ppb TOC) water, followed by sonication
11 until fully dissolved. The pH values of aqueous solutions were left unadjusted and were determined
12 using a Corning 320 pH meter. All glassware was cleaned in a KOH/EtOH base bath and rinsed
13 with water and methanol (Fisher Chemical, 99.8%) prior to use.
14
15
16
17
18
19
20
21
22
23
24
25

26 *Langmuir-Blodgett Trough:*
27

28 A custom-built Langmuir trough (52 cm × 7 cm × 0.5 cm) used previously in our group is only
29 briefly summarized here.^{12, 19, 106-111} It is made of polytetrafluoroethylene (PTFE) and equipped
30 with two computer-controlled NIMA (KSV-NIMA, Finland) PTFE barriers to restrict the
31 available surface area. A Wilhelmy balance was used to monitor the surface pressure of the
32 aqueous solution in the trough as the barriers compress molecules at the air-water interface,
33 providing surface pressure-area isotherms and therefore insight into the surface activity of the
34 molecules in solution. For example, isotherms of an aqueous PA solution, before and after
35 exposure to UV radiation, are provided in supplemental Figure S2.
36
37
38
39
40
41
42
43
44
45
46

47 A Kibron LayerX (134) dip coater attached to the custom-built Langmuir trough was used to
48 transfer molecules residing at the surface of the aqueous subphase to a solid substrate (glass slide)
49 for surface-specific species collection. The dip coater moved a clean glass slide into the aqueous
50 subphase and withdrew to its original starting position. This process was repeated for a total of 10
51
52
53
54
55
56
57
58
59
60

1
2
3 cycles, while the trough barriers compressed the surface–area such that the surface pressure was
4
5 held roughly constant. Methanol (1 mL) was used to extract the organic film collected on the glass
6
7 slide. Special care was taken to prevent solvent evaporation to avoid drying-induced chemistry.
8
9 The resulting methanol solution was analyzed with negative mode electrospray ionization–mass
10
11 spectrometry (ESI–MS). Peak assignments were made by comparing theoretical mass-to-charge
12
13 ratios for known or expected products to experimental mass-to-charge ratios. Mass accuracy for
14
15 most assignments are within ~10 ppm. Additional ESI-MS details are included in the Supporting
16
17 Information.
18
19

20
21 The aqueous subphase in Langmuir-Blodgett trough experiments consisted of 100 mM pyruvic
22
23 acid (pH ~1.8), which reflects environmental conditions and previous work.^{63, 67} Samples were
24
25 collected simultaneously from the surface, via the dip coater, and bulk, by syringe.
26
27

28 *Photochemical Studies:*

29
30 Photochemical experiments were performed by irradiating the entire aqueous sample in the
31
32 Langmuir trough with UV light. The light source consisted of Waveform Lighting light–emitting
33
34 diode strips (realUV™ LED Strip Lights; 365 nm) adhered to the trough cover, ensuring irradiation
35
36 of the entire trough surface and subphase. The spectral output of the LEDs is shown in Figure 1,
37
38 overlaid upon the absorbance spectrum of a 100 mM aqueous pyruvic acid (pH ~1.8). The LEDs
39
40 emitted radiation between 355–395 nm with a λ_{max} of ~370 nm, which overlapped with the tail end
41
42 of the photochemically relevant (n- π^*) transition of pyruvic acid as shown in Figure 1. Solar
43
44 simulators commonly used in other photochemical experiments, including aqueous solution
45
46 studies in this group,^{73, 92, 94, 99, 102, 112-113} provide radiation across a larger portion of the S₁ PA
47
48 absorption as shown in Figure 1. As such, a comparison between the bulk photochemistry of PA
49
50 irradiated with the LEDs and with the Xe arc lamp is worthwhile.
51
52
53
54
55
56
57
58
59
60

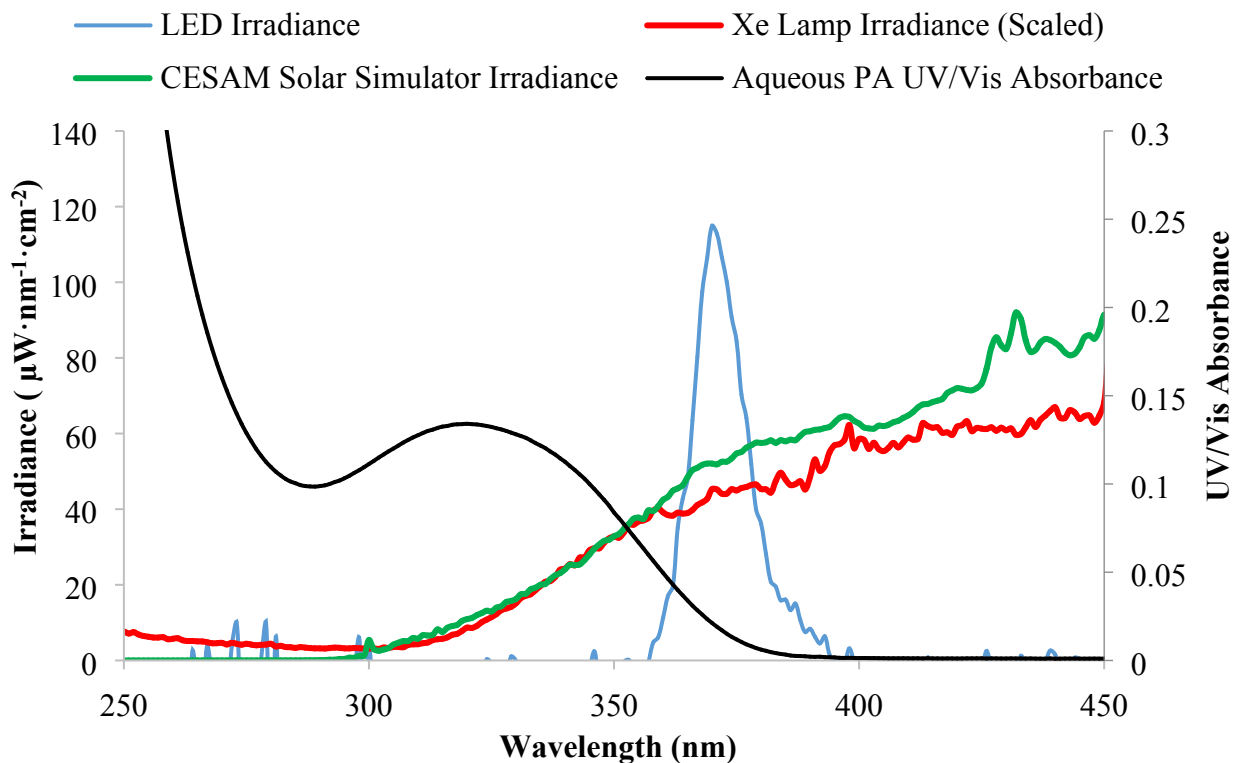


Figure 1. Comparison between the spectral outputs of the photochemical sources used in these experiments: LEDs (blue), Pyrex filtered 450 W Xe arc lamp (scaled; red), and CESAM Pyrex-filtered solar simulator (green) overlaid on the absorbance spectrum of aqueous pyruvic acid (100 mM, pH \sim 1.8; black). The Xe arc lamp output was scaled down by a factor of 11.

Light Source Comparison

Bulk, aqueous photolyses of 100 mM PA were performed with LEDs on the Langmuir trough, and with a 450 W Xe arc lamp (spectral output is shown in Figure 1) to compare photo-products obtained with the two light sources. The experimental method utilizing the 450 W Xe arc lamp is described in the section, “*Photochemical Reaction Cell*”. Each light source produced the expected major products 2,4-dihydroxy-2-methyl-5-oxohexanoic acid (DMOHA; $m/z = 175$) and dimethyltartaric acid (DMTA; $m/z = 177$) (see Table 1). Additional photolysis products include

1
2
3 acetoin ($m/z = 87$), acetolactic acid (AcLA; $m/z = 131$), and 4-carboxy-2,4-dihydroxy 2-methyl-5-
4 oxohexanoic acid (CDMOHA; $m/z = 219$). For both sources, these results were consistent with
5
6 previous studies, which have described the mechanisms of bulk aqueous PA in detail^{83-85, 93, 104, 92,}
7
8
9
10
11
12
13
14
15
16
17
18
19
20
21
22
23
24
25
26
27
28
29
30
31
32
33
34
35
36
37
38
39
40
41
42
43
44
45
46
47
48
49
50
51
52
53
54
55
56
57
58
59
60

94, 99, 102, 113 While the observed products are the same for both light sources, the normalized ion intensities of the photo-products are generally smaller in the LED photolysis than the Xe lamp photolysis. The lower intensity of the photolysis source and the limited overlap between the LED output and PA absorbance spectrum results in a slower photolysis rate, but these factors do not seem to significantly alter the photo-products observed and therefore the photochemical pathways of PA.

Table 1. Negative mode ESI-MS ion peaks of bulk aqueous 100 mM pyruvic acid after 2 hours of photolysis with two different light sources: a Xe arc lamp and LEDs.

Ion Formula, [M-H] ⁻	Assigned Structure	Theoretical m/z	Exp. m/z	Mass Diff. (ppm)	Normalized Ion Intensity (Xe lamp) ^a	Normalized Ion Intensity (LEDs) ^a
C ₃ H ₃ O ₃ ⁻	Pyruvic Acid (PA)	87.0088	87.0077	12.64	100	100
C ₄ H ₇ O ₂ ⁻	Acetoin	87.0452	87.0442	11.49	8.6	4.65
C ₅ H ₇ O ₃ ⁻	unassigned	115.0401	115.039	9.56	32.7	18.4
C ₅ H ₇ O ₄ ⁻	Acetolactic Acid (AcLA)	131.035	131.0342	6.11	36.5	9.47
C ₆ H ₇ O ₅ ⁻	PA + LA - H ₂ O	159.0299	159.0283	10.06	5.06	3.12
C ₆ H ₇ O ₆ ⁻	Parapyruvic Acid (PPA)	175.0248	175.0231	9.71	2.14	4.83
C ₇ H ₁₁ O ₅ ⁻	2,4-dihydroxy-2-methyl-5-oxohexanoic acid (DMOHA)	175.0612	175.0605	4.00	228	231
C ₆ H ₉ O ₆ ⁻	Dimethyltartaric acid (DMTA)	177.0405	177.0396	5.08	872	596

$C_8H_{11}O_7^-$	4-carboxy-2,4-dihydroxy 2-methyl-5-oxohexanoic acid (CDMOHA)	219.051	219.0501	4.11	6.15	6.82
------------------	--	---------	----------	------	------	------

^aIntensities are normalized such that the intensity of PA at $m/z = 87$ is set to 100.

Photochemical Reaction Cell

Photolysis using the solar simulator, for comparison to the LED light source, was performed in a photochemical reaction cell. An aqueous solution of pyruvic acid (100 mM; unadjusted pH ~1.8) was placed in a glass photochemical reaction cell surrounded by a temperature-controlled water bath at 20 °C. The sample was photolyzed using an unfiltered 450 W Xe arc lamp (Newport) for 2 hours with constant nitrogen sparging. Both pre- and post- 2 h photolysis aqueous pyruvic acid samples were analyzed with negative mode ESI-MS after a 1:1 dilution in methanol.

Atmospheric Simulation Chamber (CESAM)

A 4.2 m³ stainless steel atmospheric simulation chamber, CESAM (French acronym for Experimental Multiphase Atmospheric Simulation Chamber), was used here and in previous studies of gas-phase and multiphase photochemistry of PA to probe the dark chemistry and photochemistry of aqueous pyruvic acid.^{17, 79, 82, 104} We discuss the relevant experimental parameters here and a full description of the CESAM facility and analysis techniques can be found in Wang et al.¹⁰⁴ and Bregonzio-Rozier et al.¹¹⁴. In this study, an atomizer (TSI® model 3075) through a diffusion dryer (TSI®, model 3062) employed N₂ to aerosolize aqueous droplets of pyruvic acid from an aqueous solution of pyruvic acid into CESAM, conditioned to ~90% relative humidity (RH), temperature of 25 °C, and filled to ambient pressure (~1015 mbar). The nebulization process was continued until the particle mass and number concentrations (measured by a scanning mobility particle sizer) in CESAM were 20 µg/ m³ and 1 × 10⁵ #/cm³, respectively.

1
2
3 The geometric mean diameter of aqueous pyruvic acid droplets was 60 nm. Pyruvic acid droplets
4 were photolyzed by irradiation from a solar simulator consisting of three 4 kW high-pressure Xe
5 arc lamps (MH-Diffusion, MacBeam 4000), filtered by 6.5 mm thick Pyrex windows (see Figure
6
7
8
9
10 1 for CESAM solar simulator spectral output).

11
12 The gas-phase species in CESAM were tracked *in situ* with a proton transfer reaction time-of-
13 flight mass spectrometer (PTR-ToF-MS Series II, Kore Technology) that sampled the air in
14 counterflow, preventing aerosol and droplet sampling. Aqueous pyruvic acid droplets were
15 collected on filters and were analyzed post-collection with negative mode ESI-MS after extraction
16 in methanol. The data presented here are from two different CESAM experiments. We show 1)
17 the PTR-TOF-MS data (Figure 8) from an experiment that took place on 10/17/18 in which
18 droplets were nebulized from a 300 mM PA solution into CESAM filled with synthetic air and 2)
19 ESI-MS data (Table S3) of a filter collected sample from a 6/11/15 experiment in which droplets
20 were nebulized from a 100mM PA solution into CESAM filled with N₂.
21
22
23
24
25
26
27
28
29
30
31
32

33 **Results**

34
35
36 The results of two sets of distinct experiments are presented below. First, we report on the
37 chemistry and photochemistry of PA taking place at the air-water interface obtained using a
38 Langmuir-Blodgett trough and compare it to that which occurs in the bulk. Then, we compare and
39 contrast the chemistry of PA in the Langmuir trough to its chemistry in nebulized droplets using
40 an atmospheric simulation chamber, CESAM.
41
42
43
44
45
46
47

48 *Langmuir-Blodgett Studies*

49 50 Mass Spectrometry Analysis of Interfacial Pyruvic Acid

51
52
53 Prior to irradiating a 100 mM PA aqueous solution, an aliquot of the bulk solution was collected
54 and, separately, a Langmuir-Blodgett dipper and a methanol wash was used to collect molecules
55
56
57
58
59
60

residing at the surface of the solution. Both samples were analyzed after collection via negative mode ESI mass spectrometry. The resulting spectra are shown in Figure 2 and summarized in Table S2. It is immediately apparent that the sample taken from the surface contains significantly more species of relatively high molecular weight. Given that NMR results of the pyruvic acid precursor demonstrate a high degree of purity (see Figure S1) and the high molecular weight species are not seen in the bulk, these compounds are either oligomers spontaneously formed at the air-water interface and/or are formed in the bulk and then partition to the water surface where we observe them. In fact, the ability of pyruvic acid to form oligomers, such as zymonic acid, is well documented.^{37, 105}

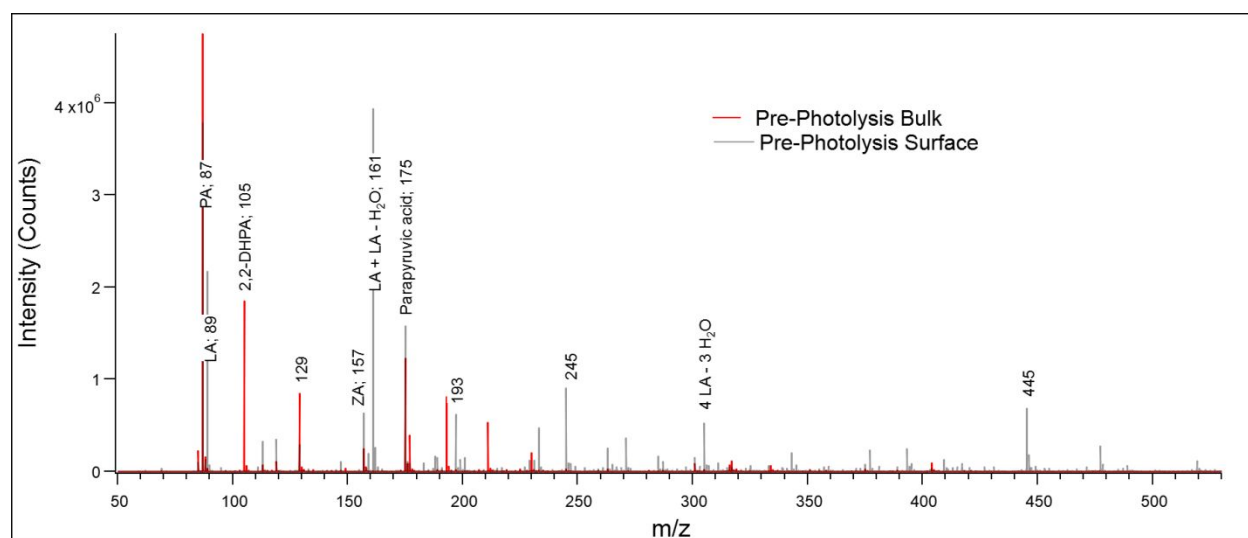


Figure 2. Negative mode ESI-MS of 100 mM PA aqueous solution sampled from the bulk (red) and the surface (transparent gray) of a Langmuir-Blodgett trough. Dark red traces result from overlap between the two defined spectra. Samples were taken immediately after the solution was deposited in the trough. The full ESI-MS ion scan range is shown to demonstrate the increased prevalence of high molecular weight species at the surface compared with the bulk.

Indeed, zymonic acid was observed at the surface and in the bulk at $m/z = 157$. Figure 3 focuses on the lower molecular weight region of Figure 2 to illustrate additional differences between the surface and bulk of the PA aqueous solution. Here, we see a strong peak at $m/z = 89$, corresponding to lactic acid (LA) or lactate, at the surface, but not in the bulk. We considered the possibility that lactic acid is merely a contamination; however, NMR of our purified PA was not able to identify any LA contamination. Additionally, in an aging experiment where 100 mM aqueous PA was allowed to sit on the trough for 3 hours (see Figure 4 and Table S1) there was LA on the surface of the solution, but not in the bulk, at time = 0 hours. After 3 hours sitting on the trough, there was a significant increase in LA at the surface but no such increase in the bulk. If LA was only a product of our collection or analysis method, the LA signal should not increase with time. Furthermore, LA is a water soluble molecule so we would expect any LA contaminant to also be observed in the bulk, yet it is only detected at the interface.

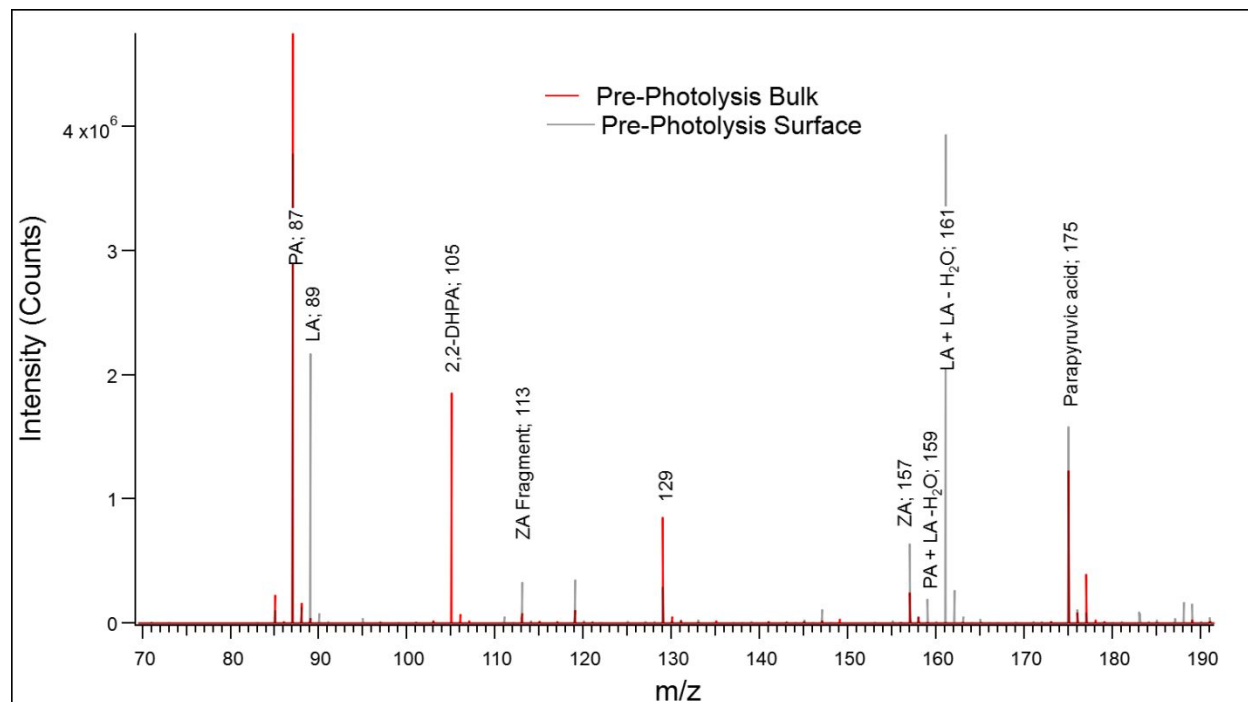


Figure 3. Negative mode ESI-MS of 100 mM PA solution sampled from the surface (transparent gray) and the bulk (red) of a Langmuir-Blodgett trough, focusing on the region of lower molecular weight. Dark red traces result from overlap between the two defined spectra. Samples were taken immediately after the aqueous solution was deposited in the trough. Pyruvic acid (PA) and/or pyruvate are the dominant species in both the surface and the bulk. Lactic acid (LA) or lactate, zymonic acid (ZA), and oligomers of PA and LA are predominantly found at the surface while the geminal diol of PA, 2,2-dihydroxypropanoic acid (2,2-DHPA) is predominantly found in the bulk. The PA dimer parapyruvic acid (PPA) appears in both the surface and bulk.

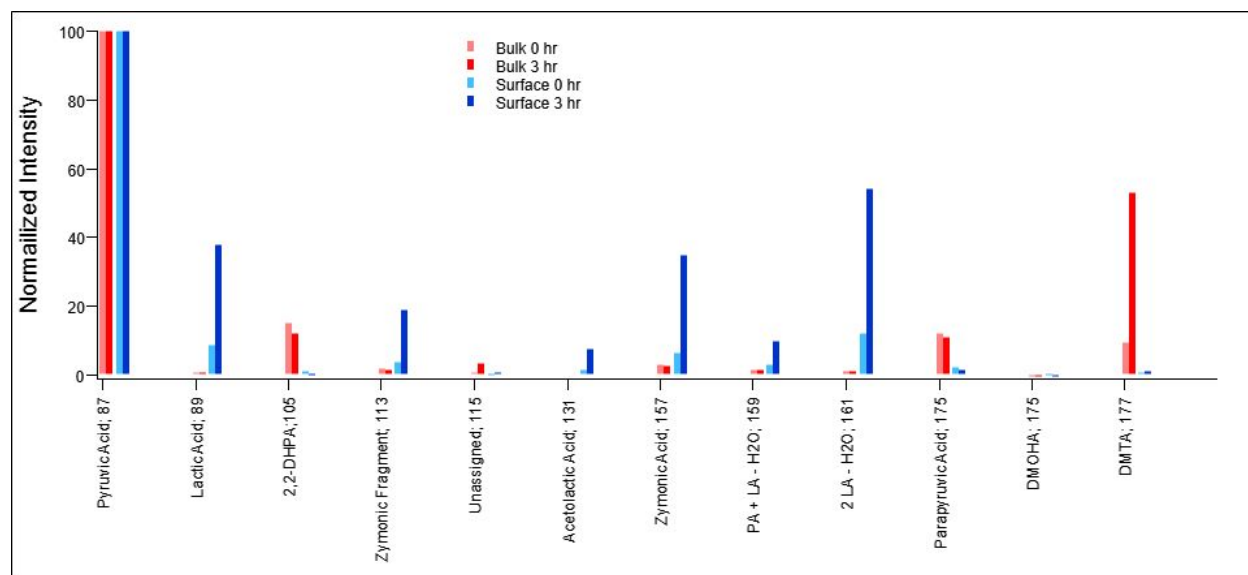


Figure 4. Behavior over time for selected ESI-MS ion peaks for Langmuir-Blodgett trough control experiments. Intensities were normalized such that the intensity of PA at $m/z = 87$ is set to 100.

The most prominent peak observed at the surface, though not in the bulk, is at $m/z = 161$ which may correspond to the condensation product of two lactic acid monomers. At $m/z = 159$ we also

1
2
3 observe the presence of what may be PA + LA – H₂O. In fact, as listed in Table S2, many of the
4
5 higher molecular weight species shown in Figure 2 correspond to the myriad possible oligomers
6
7 potentially formed from combinations of LA and PA molecules and the requisite loss of water
8
9 molecules.
10

11
12 Another interesting difference between the aqueous PA surface and bulk reaction environments
13
14 is revealed by the peak found only in the bulk at $m/z = 105$: the diol form of PA. Likely more
15
16 soluble than the keto form due to its additional –OH groups and probably less likely to form at or
17
18 partition to the surface given the water-restricted nature of the interface, it seems reasonable the
19
20 diol is not observed at the surface. Furthermore, we do not expect that washing the diol in
21
22 methanol, as performed on all samples collected from the water surface, would force the diol back
23
24 into the keto form of PA.¹¹⁵⁻¹¹⁶
25
26

27 28 Photochemistry of Pyruvic Acid at the Surface of Water 29

30
31 A Langmuir-Blodgett trough was coupled to photochemistry-inducing LEDs and used to
32
33 photolyze aqueous PA solutions. After irradiating a 100 mM solution of aqueous PA in the trough
34
35 for 3 hours, an aliquot of the bulk solution was collected from the trough and a Langmuir-Blodgett
36
37 dipper was used to collect molecules residing at the surface of the solution. Negative mode ESI-
38
39 MS was used to analyze both samples and the results are shown in Figure 5 and summarized in
40
41 Table S2 and Figure 6.
42
43
44
45
46
47
48
49
50
51
52
53
54
55
56
57
58
59
60

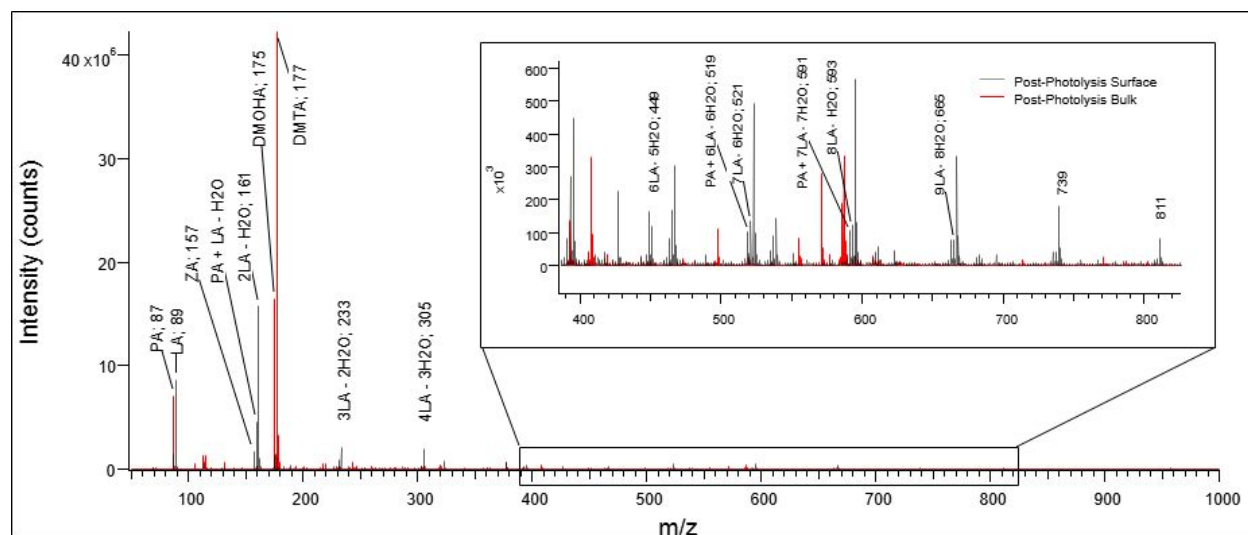


Figure 5. Negative mode ESI-MS of 100 mM aqueous PA sampled from the Langmuir-Blodgett trough surface (transparent gray) and bulk (red) after 3 hours of irradiation. Dark red traces result from overlap between the two defined spectra.

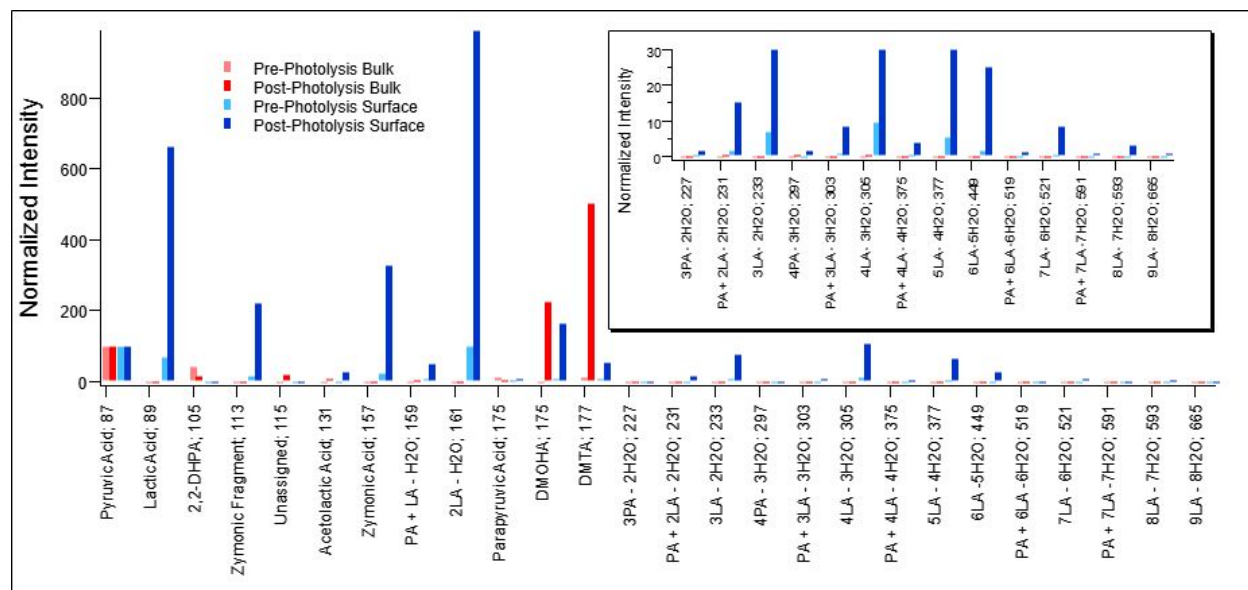


Figure 6. Behavior over time for selected ESI-MS ion peaks of 100 mM PA before and after photolysis, sampled in the bulk and on the solution surface. Intensities were normalized such that the intensity of PA at $m/z = 87$ is set to 100.

At the surface, pre- and post-photolysis, the most prominent signals arise from PA ($m/z = 87$), LA ($m/z = 89$), and the host of PA, LA, and PA/LA oligomers at $m/z = 157$ (ZA), 159, 161, 231, 303, etc. These oligomeric species are more prevalent after irradiation. Zymonic acid is well known to form in the dark¹⁰⁵, but these experiments also show dark production of LA and other oligomers. Additionally, the formation of the well-documented aqueous PA photo-products^{37, 63, 80, 90, 92, 97, 99, 101-102, 113} is observed on the surface post-irradiation, the most prominent of which include acetolactic acid ($m/z = 131$), DMOHA ($m/z = 175$), and DMTA ($m/z = 177$). The mechanism for the formation of these species in bulk aqueous phase has been previously reported.^{17, 63, 73, 92, 99}

Figure 7 compares the post-photolysis mass spectrum taken from the bulk to that which was taken from the surface of a Langmuir-Blodgett trough. Though LA is a well-known photolysis product of PA in aqueous solution, the most striking differences in the post photolysis mass spectra are the observation of LA and PA/LA oligomers at the surface but not in the bulk solution. In the bulk, the major species are the photo-products DMOHA and DMTA. While they are also observed at the interface, the relative concentrations are much greater in the bulk than at the surface.

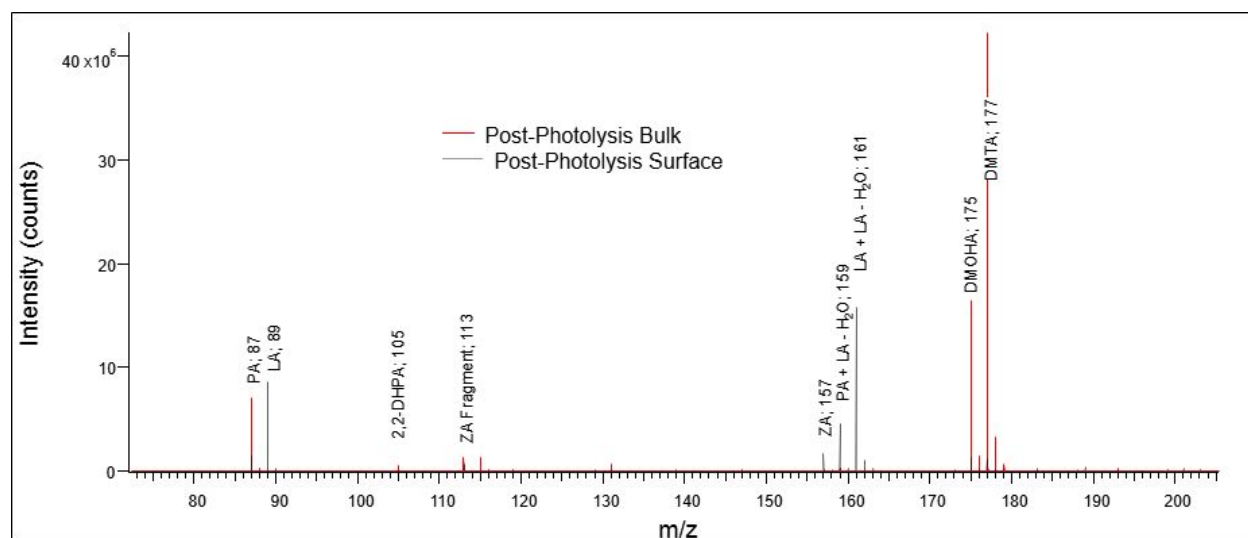


Figure 7. Negative mode ESI-MS of a 100 mM PA aqueous solution after 3 hours of irradiation with samples taken from the surface (transparent gray) and bulk (red) of a Langmuir-Blodgett trough. Dark red traces result from overlap between the two defined spectra. The expected photolysis products 2,4-dihydroxy-2-methyl-5-oxohexanoic acid (DMOHA) and dimethyltartaric acid (DMTA) are found primarily in the bulk. Zymonic acid (ZA), lactic acid (LA), and oligomers of PA and LA are found primarily at the surface.

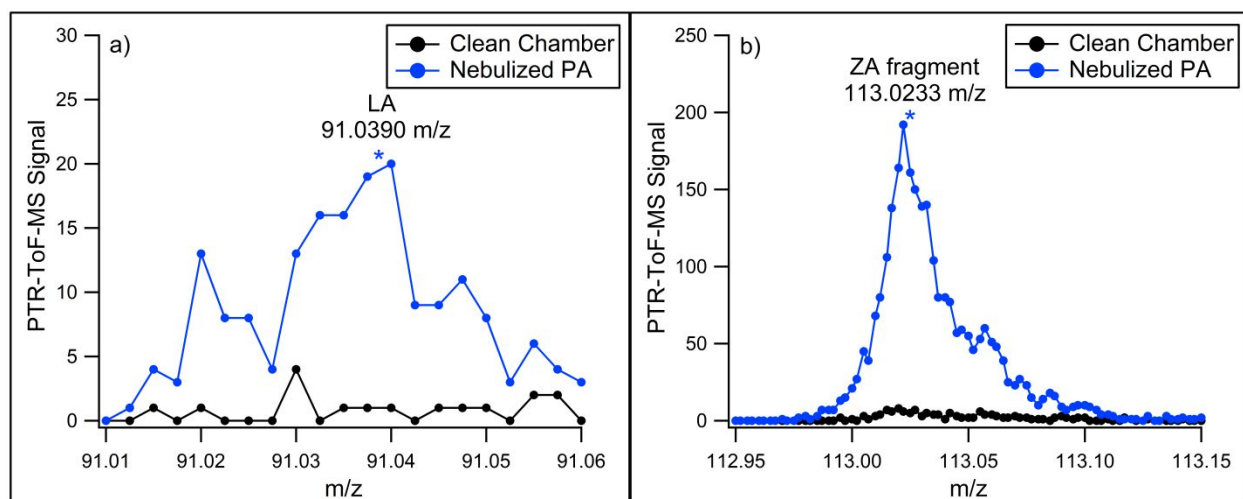
Overall, the chemistry and photochemistry of PA at the air-water interface is defined by the formation of lactic acid and/or lactate and several oligomers comprising various ratios of PA to LA monomers. The production of expected PA photo-products such as DMOHA and DMTA may be limited at the surface compared to the bulk.

Simulation Chamber (CESAM) Studies of Nebulized Aqueous PA Microdroplets

Aqueous PA droplets in CESAM, formed via nebulization of 100 mM aqueous PA, were filter-collected before photolysis and analyzed with ESI-MS. Results were compared to ESI-MS measurements of the bulk sample prepared in the photochemical reaction cell experiment before photolysis and can be seen in Table S3. The relative amounts of some species were much larger in the PA droplets than observed in the bulk including acetoin ($m/z = 87$), lactic acid (LA; $m/z = 89$), zymonic acid (ZA; $m/z = 157$), PA + LA - H₂O ($m/z = 159$), and parapyruvic acid (PPA; $m/z = 175$). These results suggest that dark chemistry not seen in bulk aqueous solutions can occur in PA droplets which, collectively, have a large surface area to volume ratio.

Support for the formation of lactic and zymonic acids at the droplet surface can be seen in Figure 8, where PTR-ToF-MS signals of their ions are shown as PA is nebulized into CESAM. The zymonic acid fragment signal ($[M + H - H_2O - CO]^+$ at $m/z = 113$)¹⁷ greatly increased as PA was nebulized into the chamber. The fragment signal at $m/z = 113$ is used as a marker for zymonic acid

1
2
3 instead of its parent peak at $m/z = 159$ as the former is seen with larger intensity. However, both
4
5 PTR-ToF-MS ion signals representative of the acid follow the same time trend. Lactic acid ($m/z =$
6
7 91) also increased during PA nebulization, though not as significantly. Neither of these PTR-ToF-
8
9 MS signals were observed in the gas-phase dark aging experiments of PA⁷⁹, indicating the droplets,
10
11 and more specifically their surface^{14, 45}, are necessary for this dark production. The particle
12
13 number and mass concentration of PA in the multiphase nebulized experiment were 10^5 particles
14
15 cm^{-3} and $20 \mu\text{g m}^{-3}$, respectively, with a number weighted mean geometric diameter of 60 nm. The
16
17 average surface area and surface to volume ratio of a PA particle in the experiment were 0.011
18
19 μm^2 and 0.1 nm^{-1} , respectively.
20
21
22
23



24
25
26
27
28
29
30
31
32
33
34
35
36
37
38
39
40 **Figure 8.** PTR-ToF-MS ion peaks for a) lactic acid (LA, $m/z = 91.0390$) and b) zymonic acid (ZA;
41
42 $[\text{M} + \text{H} - \text{H}_2\text{O} - \text{CO}]^+$ $m/z = 113.0233$) fragment in the nebulized pyruvic acid CESAM experiment.
43
44 The mass spectra are shown as lines with solid circle markers and are colored black for the clean
45
46 chamber and blue for nebulized pyruvic acid in the chamber.
47
48

49 Discussion

50
51
52 A previous study of the multiphase chemistry of pyruvic acid observed products such as zymonic
53
54 acid not previously seen in PA photochemistry, and proposed that the surface of aqueous droplets
55
56
57
58
59
60

1
2
3 plays a key role in their production¹⁷ while a different study noted that PA at interface is more
4 likely to photochemically form HMWCs than PA in the bulk.³⁷ Chemistry leading to
5 oligomerization is especially important for atmospheric chemistry and abiotic synthesis in both
6 contemporary and prebiotic contexts.^{11, 27, 112-113, 117-120} Here, we used a combination of Langmuir-
7 Blodgett trough experiments and simulation chamber studies to investigate the photochemical and
8 dark chemistry of pyruvic acid which may occur at the surface of water, leading to products not
9 found in the bulk, aqueous phase. Additionally, chemistry in bulk water can lead to products which
10 partition to the surface and are collected and analyzed in this work. Both outcomes lead to a
11 modified chemical environment at the air-water interface.
12
13
14
15
16
17
18
19
20
21
22

23
24 Although pyruvic acid is a relatively soluble organic molecule, it has a higher than expected
25 surface activity given its solubility of 10^6 mg/L or 11.4 M.⁴⁵ Gordon et al.⁴⁵ showed through
26 computational studies that pyruvic acid, as well as parapyruvic acid and zymonic acid dimers, have
27 a positive surface excess indicating that all three forms partition to the surface to some extent.
28 These computational results are confirmed by vibrational sum frequency generation data also
29 found in Gordon et al.⁴⁵ and by the MS data we present here.
30
31
32
33
34
35
36

37
38 A comparison between surface products obtained in the Langmuir-Blodgett trough and those
39 acquired from droplet experiments in the CESAM atmospheric chamber can help illuminate the
40 role of the air-water interface in microdroplet chemistry. Microdroplets produced in the simulation
41 chamber had a number density of 10^5 particles cm^{-3} with an average diameter of 60 nm, presenting
42 a collective surface area in the simulation chamber of 4.8×10^{-3} m^2 . The ratio of surface area to bulk
43 volume increases by more than a factor of one million in going from the trough to a droplet,
44 providing a unique ability to differentiate surface and bulk chemistry. We expect both experiments
45
46
47
48
49
50
51
52
53
54
55
56
57
58
59
60

1
2
3 to provide enough surface area to reliably observe any product discrepancies between surface and
4
5 bulk experiments and attribute those differences to the air-water interface.
6

7
8 Information on the surface composition and reactivity of PA is obtained in this study with surface
9
10 sensitive methods. Specifically, we utilized a Langmuir trough equipped with a Blodgett dipper to
11
12 sample species directly from solution surfaces while the bulk of the solution was separately
13
14 sampled, allowing for an internal comparison between the two environments. LEDs were fitted to
15
16 the trough to study the photochemistry of PA at the air-water interface. This guaranteed that the
17
18 entire surface area was illuminated such that efficient and uniform photolysis of the solution was
19
20 achieved.
21
22

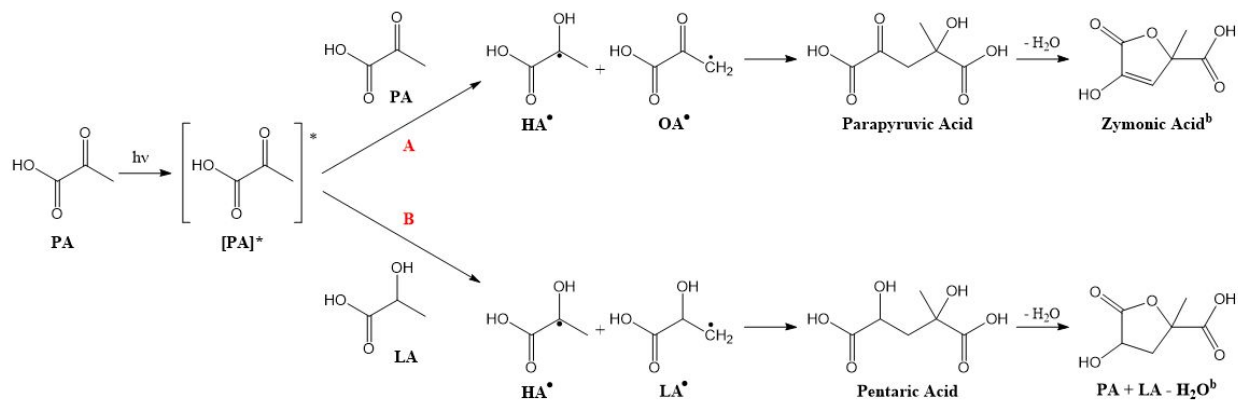
23
24 Although we study the interfacial chemistry of PA on flat Langmuir troughs, many of the
25
26 systems to which we would like to compare and apply our insight into interfacial chemistry are
27
28 microdroplets or atmospheric aerosols. Given the size of those systems (diameter $\sim 1 \mu\text{m}$) and
29
30 molecular length of most organic molecules of a few Angstroms, the surface area of a droplet is
31
32 large compared to the area occupied by a molecule ($\sim 10^7$ times larger). Consequently, the surface
33
34 is effectively flat and any effects caused by the curvature of the interface on the reaction
35
36 mechanism can be neglected.
37
38

39
40 Indeed, nebulized aqueous PA solution in the simulation chamber CESAM, sampled in real
41
42 time by PTR-ToF-MS and off-line by ESI-MS of filter samples, largely exhibited the same
43
44 composition as that observed on the flat trough surface, supporting our assertion that the Langmuir
45
46 trough can adequately model environmental interfaces. Specifically, lactic acid/lactate and
47
48 zymonic acid were detected both in CESAM aerosol experiments and in our surface trough
49
50 experiments in the absence of irradiation. We also saw substantial formation of other oligomers at
51
52 the surface of the trough experiments, ostensibly from a combination of lactic and pyruvic acid
53
54
55
56
57
58
59
60

1
2
3 monomers. The most prominent of these oligomers are found at $m/z = 161$ and 159 , possibly
4 corresponding to $LA + LA - H_2O$ and $PA + LA - H_2O$, respectively, but a series of these oligomers
5
6 comprised of several PA or LA monomers are observed. Fu et al.³⁷ also observed $m/z = 159$ in
7
8 their photochemical PA experiments and suggested it is formed via intramolecular esterification
9
10 induced by the drying of their bulk liquid sample. They did not detect $m/z = 161$ or lactic acid.
11
12
13

14 We propose the $m/z = 159$ peak is a $PA + LA - H_2O$ dimer that may be formed by a similar
15
16 mechanism as zymonic acid, as shown in Scheme 1. It has been proposed elsewhere that after
17
18 irradiation, the excited pyruvic acid molecule may abstract hydrogen from the methyl group on
19
20 another PA molecule forming two radicals which combine to form parapyruvic acid ($m/z = 175$).⁹⁹
21
22 ¹⁰² Parapyruvic acid may then dehydrate to form another detected product ($m/z = 157$). We
23
24 propose that the $PA + LA - H_2O$ dimer may form when the excited PA molecule abstracts
25
26 hydrogen from a LA molecule forming radicals such as HA^\bullet and LA^\bullet which then combine and
27
28 dehydrate to form the dimer product ($m/z = 159$). Likely structures for both the $PA + PA - H_2O$
29
30 and $PA + LA - H_2O$ dimers are shown in Scheme 1. Additional possible structures are shown in
31
32 the SI, Figure S4. Regardless of the exact mechanism for formation, neither lactic acid nor the
33
34 resulting oligomers are observed in the bulk of the trough solution, suggesting this phenomenon
35
36 may be surface specific. In contrast, the hydrated, diol form of pyruvic acid is only found in the
37
38
39
40
41
42
43
44
45
46
47
48
49
50
51
52
53
54
55
56
57
58
59
60

Scheme 1. Proposed mechanism for $PA + LA - H_2O$ dimer formation (pathway B) as compared
to the proposed mechanism for Zymonic Acid^a, i.e. $2 PA - H_2O$, dimer formation^{99, 102} (pathway
A).



^aZA is a known product under both dark and photochemical reactions of PA.^{17, 105}

^bThe final product structures shown here are one of multiple possible stereoisomers for the PA + PA - H₂O and PA + LA - H₂O dimers. See the Supplemental Information, Figure S4 for other potential product structures.

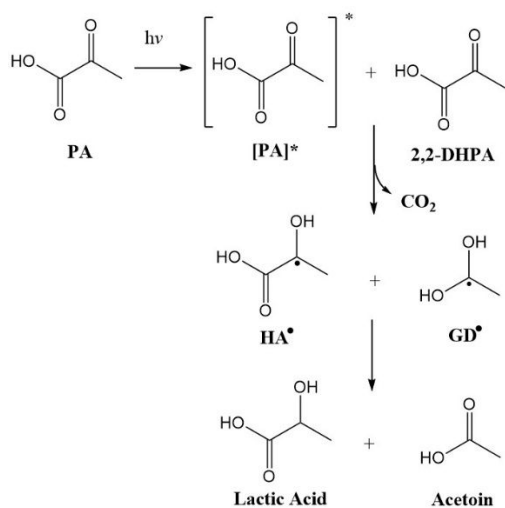
Zymonic acid has previously been observed as a product of PA photolysis.^{17, 37} ZA is formed by the combination of two pyruvic acid molecules with the elimination of water, as shown in Scheme 1 pathway A. Since molecules at the air-water interface are partially solvated, they experience a water restricted environment so dehydration, and therefore dimer formation, is likely enhanced at the surface compared to the bulk. Indeed, Reed Harris et al.¹⁷ observed its formation in aqueous PA droplets and suggested it may be a surface process given it had not been detected in bulk PA photolysis, which we corroborate. Fu et al.³⁷ also observed photochemical production of ZA in both their interfacial and bulk experiments, but suggest its presence in their bulk liquid phase samples to result from drying of the sample prior to analysis. Zymonic acid has also been previously observed to form from aqueous PA in the dark,¹⁰⁵ but here we present for the first time data which shows its presence on the surface of an uncontaminated aqueous PA solution and not in the bulk.

1
2
3 Xiao Sui et al. have used *in situ* liquid Time-of-Flight Secondary Ion Mass Spectrometry (ToF-
4 SIMS) to study glyoxal oxidation at the surface of water with hydrogen peroxide.^{55, 121} When they
5
6 compare their liquid ToF-SIMS spectrum to a ToF-SIMS spectrum of a dried glyoxal/peroxide
7
8 solution, they find several differences. Namely, the dried sample exhibited more dehydrated
9
10 oligomers, while the oligomers observed on the liquid surface tended to be hydrated. We
11
12 acknowledge our dipper experiments could be susceptible to an analogous drying effect on the
13
14 glass slide which enhances the formation of the condensation products, like zymonic acid, we
15
16 present here. However, having taken steps to mitigate drying on the slide, having presented an
17
18 aging experiment in the Langmuir trough (where drying is negligible) in which the condensation
19
20 products appear to grow in over time, and having observed zymonic acid in an *in situ* droplet
21
22 experiment, it is likely that at least some of the observed oligomers are being formed at the water
23
24 interface prior to our disruption of the system. Regardless, drying may be important to atmospheric
25
26 aerosol chemistry, as aerosols experience a wide range of humidity and temperature over the
27
28 course of their life cycle.
29
30
31
32
33
34

35 Lactic acid, however, is a known product of pyruvic acid photolysis, as shown in Scheme 2.^{63,}
36
37 ^{92, 99} Though, here, we also observe its formation in the absence of irradiation. In order to rule out
38
39 lactic acid as a mere contaminant, we examined NMR data of our purified PA as shown in Figure
40
41 S1 and did not detect any signal where known chemical shifts of lactic acid would be present. The
42
43 reduction of pyruvate to lactate in microdroplets has been reported by Lee et al.¹⁴ This work
44
45 implicated the role of the droplet surface, although the solutions in Lee et al.¹⁴ were more dilute
46
47 than those used in the present study. The presence of LA or lactate at the surface but not in the
48
49 bulk in our experiments can be examined in light of the reduction potentials for pyruvate. Bulk
50
51 aqueous potentials for the reduction of pyruvate to lactate and oxidation of OH⁻ ions to release
52
53
54
55
56
57
58
59
60

electrons are -0.185 V^{122} and 2.72 V^{123} , respectively. We note that these potentials are bulk values which may change at the air-water interface where water is much more likely to autoionize.¹²⁴⁻¹²⁶ However, these values are well within estimates for the surface potential of water. It has been estimated that a 5 \AA air-water interface may create a potential of approximately 3 V based on previous studies, which exceeds the potential necessary to reduce pyruvate.¹²⁷⁻¹²⁸ Other work from Chamberlayne et al.²⁰ and Xiong et al.²¹ has shown that the electric double layer of charge in water microdroplets will produce an electric field at the surface on the order of 10^7 V/cm , corresponding to a surface potential of 3.63 V . Although this work utilizes flat surfaces in addition to droplets, the electric double layer will also exist on a flat surface and it is therefore reasonable to expect similar electric fields. Xiong et al.²¹ posit that strong fields, like the one they observe, may support spontaneous reduction at the air-water interface.

Scheme 2. Photochemical pathway for lactic acid production from aqueous pyruvic acid.⁶³



^aIn this case it has been proposed that the excited PA molecule hydrogen abstracts from the acid group of the diol form of PA, 2,2-DHPA, which subsequently loses the CO_2 group forming the HA^\bullet and GD^\bullet radicals. These radicals then form acetic and lactic acids.

1
2
3 When we photolyzed aqueous PA solutions, we detected in the bulk the major species predicted
4 by known solution-phase PA photolysis mechanisms, including acetolactic acid, DMTA, and
5 DMOHA.^{92, 99} These species were also present at the surface, but were overshadowed by lactic
6 acid and the abundance of LA and PA oligomers. Given that LA and other oligomers were
7 observed in the dark and are also known to form photochemically, it is difficult to quantitatively
8 assess contributions for each process. Ultimately, however, it is clear that the air-water interface
9 allows for efficient concentration of surface-active oligomers relative to the bulk aqueous solution
10 in both dark and photochemical settings. This generalization is supported by Surface Area –
11 Pressure Isotherms performed here and shown in the SI (Figure S2), where the surface activity is
12 clearly enhanced following photolysis. Additionally, nebulized aqueous PA droplets have been
13 shown to become more viscous and grow in size upon photolysis, indicating similar
14 polymerization reactions occurred.¹⁷

30 **Conclusions**

31
32
33 The results of the chemistry of PA presented above demonstrate that chemistry at the air-water
34 interface can be very different than in bulk water, with a strong propensity for oligomer formation
35 at the surface of water. In this study, we used a soluble surfactant, pyruvic acid, which has been
36 well studied previously in both gas and bulk aqueous solutions, with and without exposure to
37 irradiation. Here, we investigated its chemistry at the air-water interface using both flat surfaces
38 (Langmuir-Blodgett troughs) and nebulized microdroplets in an atmospheric simulation chamber
39 (CESAM). A comparison of products found at the surface of water and in bulk aqueous solution
40 clearly shows a difference in surface-enhanced products formed under dark and light conditions.
41 Results from dark experiments show that lactic acid/lactate and zymonic acid, a pyruvic acid
42 dimer, are both observed preferentially at the air-water interface. Additionally, we detected a series
43
44
45
46
47
48
49
50
51
52
53
54
55
56
57
58
59
60

1
2
3 of higher molecular weight oligomers consisting of mixed monomer units of pyruvic and lactic
4 acids further indicating the tendency of oligomers to reside at the surface of water. When
5 photochemistry is performed we find that DMTA and DMOHA are more prevalent relative to PA
6 in the bulk than on the surface while other products including LA, LA oligomers, and ZA are
7 observed at the surface.
8
9

10
11
12
13
14 Due to the prevalence of pyruvic acid in a variety of environments including the modern
15 atmosphere, prebiotic Earth, and cellular systems the differences in its chemistry and
16 photochemistry at the air-water interface compared to bulk solution may be important. A previous
17 study has shown the impact that mechanistic studies of condensed phase aqueous pyruvic acid
18 could have on atmospheric modelling.⁶³ It showed that not only did aqueous photolysis rates scale
19 differently than gas-phase rates, a fact not previously accounted for in atmospheric models, but the
20 types of products produced in the aqueous phase led to secondary organic aerosols (SOAs).
21 Another study showed PA at the interface is susceptible to drying induced chemistry which differs
22 from bulk photochemistry and produces compounds capable of contributing to aqSOA
23 formation.³⁷ It is likely that the added detail of pyruvic acid chemistry, specifically at the air-water
24 interface, will impact modeling both in regards to the pyruvic acid depletion rates and the
25 formation of SOAs. Furthermore, the production of lactic acid from pyruvic acid is strikingly
26 similar to the role of pyruvic acid in the metabolic cycle. Today, this reduction occurs with enzyme
27 catalysis. However, this work may support the Lee et al.¹⁴ postulate that this could be a route for
28 prebiotic metabolism. Finally, as Lee et al.¹⁴ also mentions, the fact that most pyruvic acid
29 chemistry occurs in cells where interfaces are ubiquitous indicates that these studies could have
30 significant implications for cellular chemistry. Regardless, in both modern and prebiotic contexts
31
32
33
34
35
36
37
38
39
40
41
42
43
44
45
46
47
48
49
50
51
52
53
54
55
56
57
58
59
60

1
2
3 the surface of water may be an important catalyst for generating chemically complex systems in
4
5 the natural environment.
6

7 **Supporting Information**

8
9
10 Analytical Techniques and Instrument Parameters: NMR Analysis and Mass Spectrometry;
11 Representative ^1H NMR spectrum (400 MHz) of purified pyruvic acid in DMSO- d_6 ; Surface
12 Pressure-Area Isotherms of an aqueous solution of 100 mM PA before and after UV irradiation;
13 Negative mode ESI-MS of a zymonic acid standard; Negative mode ESI-MS ion peaks for
14 Langmuir-Blodgett trough control experiments; Negative mode ESI-MS ion peaks of 100 mM
15 aqueous PA before and after photolysis, sampled in the bulk and on the solution surface of a
16 Langmuir-Blodgett trough; ESI-MS Comparison of Pre-Photolysis Aqueous Bulk PA Solution
17 and PA Droplets; Potential structures for A) PA + PA - H $_2$ O, $m/z = 157$, and B) PA + LA - H $_2$ O,
18 $m/z = 159$, dimers.
19
20
21

22 **Acknowledgements**

23
24
25
26 This work was funded by the U. S. Army Research Office under the grant no. ARO
27
28 W911NF1710115 and the National Science Foundation grant no. CHE 1611107. A.M.D. also
29
30 acknowledges funding from the National Science Foundation Graduate Research Fellowship under
31
32 Grant No. DGE 1650115. We also thank the University of Colorado at Boulder Central Analytical
33
34 Laboratory Mass Spectrometry Core Facility for use of their instruments. The authors gratefully
35
36 thank CNRS-INSU for supporting CESAM as a national facility and AERIS datacenter (aeris-
37
38 data.fr) for hosting simulation chamber data.
39
40
41

42 **References**

- 43
44
45 1. Carslaw, K. S.; Lee, L. A.; Reddington, C. L.; Pringle, K. J.; Rap, A.; Forster, P. M.; Mann, G. W.;
46 Spracklen, D. V.; Woodhouse, M. T.; Regayre, L. A.; Pierce, J. R., Large contribution of natural aerosols to
47 uncertainty in indirect forcing. *Nature* **2013**, *503* (7474), 67-71.
48 2. Donaldson, D. J.; Vaida, V., The influence of organic films at the air-aqueous boundary on
49 atmospheric processes. *Chemical Reviews* **2006**, *106* (4), 1445-61.
50 3. Ellison, G. B.; Tuck, A. F.; Vaida, V., Atmospheric processing of organic aerosols. *Journal of*
51 *Geophysical Research: Atmospheres* **1999**, *104* (D9), 11633-11641.
52 4. Ervens, B.; Carlton, A. G.; Turpin, B. J.; Altieri, K. E.; Kreidenweis, S. M.; Feingold, G., Secondary
53 organic aerosol yields from cloud-processing of isoprene oxidation products. *Geophysical Research*
54 *Letters* **2008**, *35* (2), 5.
55
56
57
58
59
60

- 1
 - 2
 - 3
 - 4
 - 5
 - 6
 - 7
 - 8
 - 9
 - 10
 - 11
 - 12
 - 13
 - 14
 - 15
 - 16
 - 17
 - 18
 - 19
 - 20
 - 21
 - 22
 - 23
 - 24
 - 25
 - 26
 - 27
 - 28
 - 29
 - 30
 - 31
 - 32
 - 33
 - 34
 - 35
 - 36
 - 37
 - 38
 - 39
 - 40
 - 41
 - 42
 - 43
 - 44
 - 45
 - 46
 - 47
 - 48
 - 49
 - 50
 - 51
 - 52
 - 53
 - 54
 - 55
 - 56
 - 57
 - 58
 - 59
 - 60
5. Ruiz-Lopez, M. F.; Francisco, J. S.; Martins-Costa, M. T.; Anglada, J. M., Molecular reactions at aqueous interfaces. *Nature Reviews Chemistry* **2020**, 1-17.
6. Stevens, B.; Feingold, G., Untangling aerosol effects on clouds and precipitation in a buffered system. *Nature* **2009**, *461* (7264), 607-13.
7. Tang, M.; Cziczo, D. J.; Grassian, V. H., Interactions of water with mineral dust aerosol: Water adsorption, hygroscopicity, cloud condensation, and ice nucleation. *Chemical Reviews* **2016**, *116* (7), 4205-59.
8. Zhong, J.; Kumar, M.; Anglada, J. M.; Martins-Costa, M. T. C.; Ruiz-Lopez, M. F.; Zeng, X. C.; Francisco, J. S., Atmospheric spectroscopy and photochemistry at environmental water interfaces. *Annual Review of Physical Chemistry, Vol 70* **2019**, *70*, 45-69.
9. George, C.; Ammann, M.; D'Anna, B.; Donaldson, D. J.; Nizkorodov, S. A., Heterogeneous photochemistry in the atmosphere. *Chemical Reviews* **2015**, *115* (10), 4218-4258.
10. Banerjee, S.; Gnanamani, E.; Yan, X.; Zare, R. N., Can all bulk-phase reactions be accelerated in microdroplets? *Analyst* **2017**, *142* (9), 1399-1402.
11. Dobson, C. M.; Ellison, G. B.; Tuck, A. F.; Vaida, V., Atmospheric aerosols as prebiotic chemical reactors. *Proceedings of the National Academy of Sciences* **2000**, *97* (22), 11864-8.
12. Griffith, E. C.; Vaida, V., In situ observation of peptide bond formation at the water-air interface. *Proceedings of the National Academy of Sciences* **2012**, *109* (39), 15697-701.
13. Lee, J. K.; Banerjee, S.; Nam, H. G.; Zare, R. N., Acceleration of reaction in charged microdroplets. *Quarterly Reviews of Biophysics* **2015**, *48* (4), 437-44.
14. Lee, J. K.; Samanta, D.; Nam, H. G.; Zare, R. N., Micrometer-sized water droplets induce spontaneous reduction. *Journal of the American Chemical Society* **2019**, *141* (27), 10585-10589.
15. Marsh, B. M.; Iyer, K.; Cooks, R. G., Reaction acceleration in electrospray droplets: Size, distance, and surfactant effects. *Journal of The American Society for Mass Spectrometry* **2019**, *30* (10), 2022-2030.
16. Nam, I.; Lee, J. K.; Nam, H. G.; Zare, R. N., Abiotic production of sugar phosphates and uridine ribonucleoside in aqueous microdroplets. *Proceedings of the National Academy of Sciences* **2017**, *114* (47), 12396-12400.
17. Reed Harris, A. E.; Pajunoja, A.; Cazaunau, M.; Gratien, A.; Pangu, E.; Monod, A.; Griffith, E. C.; Virtanen, A.; Doussin, J. F.; Vaida, V., Multiphase photochemistry of pyruvic acid under atmospheric conditions. *Journal of Physical Chemistry A* **2017**, *121* (18), 3327-3339.
18. Rossignol, S.; Tinel, L.; Bianco, A.; Passananti, M.; Brigante, M.; Donaldson, D. J.; George, C., Atmospheric photochemistry at a fatty acid-coated air-water interface. *Science* **2016**, *353* (6300), 699-702.
19. Griffith, E. C.; Vaida, V., Ionization state of L-phenylalanine at the air-water interface. *Journal of the American Chemical Society* **2013**, *135* (2), 710-716.
20. Chamberlayne, C. F.; Zare, R. N., Simple model for the electric field and spatial distribution of ions in a microdroplet. *The Journal of chemical physics* **2020**, *152* (18), 184702.
21. Xiong, H.; Lee, J. K.; Zare, R. N.; Min, W., Strong electric field observed at the interface of aqueous microdroplets. *The journal of physical chemistry letters* **2020**, *11* (17), 7423-7428.
22. Seinfeld, J. H.; Pandis, S. N., *Atmospheric chemistry and physics: From air pollution to climate change*. John Wiley & Sons: 2016.
23. Finlayson-Pitts, B. J.; Pitts Jr, J. N., *Chemistry of the upper and lower atmosphere: Theory, experiments, and applications*. Elsevier: 1999.
24. Donaldson, D.; Valsaraj, K. T., Adsorption and reaction of trace gas-phase organic compounds on atmospheric water film surfaces: A critical review. *Environmental science & technology* **2010**, *44* (3), 865-873.

- 1
2
3 25. Evrens, B.; Turpin, B.; Weber, R., Secondary organic aerosol formation in cloud droplets and
4 aqueous particles (aqsoa): A review of laboratory, field and model studies. *Atmospheric Chemistry &*
5 *Physics Discussions* **2011**, *11* (8).
- 6 26. Pezzotti, S.; Galimberti, D. R.; Gaigeot, M.-P., 2D H-bond network as the topmost skin to the air–
7 water interface. *The journal of physical chemistry letters* **2017**, *8* (13), 3133-3141.
- 8 27. Griffith, E. C.; Tuck, A. F.; Vaida, V., Ocean-atmosphere interactions in the emergence of
9 complexity in simple chemical systems. *Accounts of Chemical Research* **2012**, *45* (12), 2106-2113.
- 10 28. Mompean, C.; Marin-Yaseli, M. R.; Espigares, P.; Gonzalez-Toril, E.; Zorzano, M. P.; Ruiz-Bermejo,
11 M., Prebiotic chemistry in neutral/reduced-alkaline gas-liquid interfaces. *Scientific Reports* **2019**, *9*, 12.
- 12 29. Powner, M. W.; Gerland, B.; Sutherland, J. D., Synthesis of activated pyrimidine ribonucleotides
13 in prebiotically plausible conditions. *Nature* **2009**, *459* (7244), 239-42.
- 14 30. Tuck, A., The role of atmospheric aerosols in the origin of life. *Surveys in Geophysics* **2002**, *23* (5),
15 379-409.
- 16 31. Tuck, A. F., Proposed empirical entropy and gibbs energy based on observations of scale
17 invariance in open nonequilibrium systems. *The Journal of Physical Chemistry A* **2017**, *121* (35), 6620-
18 6629.
- 19 32. Mason, B., Bursting of air bubbles at the surface of sea water. *Nature* **1954**, *174* (4427), 470-471.
- 20 33. Tuck, A. F., Gibbs free energy and reaction rate acceleration in and on microdroplets. *Entropy*
21 **2019**, *21* (11), 1044.
- 22 34. Alpert, P. A.; Ciuraru, R.; Rossignol, S.; Passananti, M.; Tinel, L.; Perrier, S.; Dupart, Y.; Steimer, S.
23 S.; Ammann, M.; Donaldson, D. J., Fatty acid surfactant photochemistry results in new particle
24 formation. *Scientific Reports* **2017**, *7* (1), 1-11.
- 25 35. Altieri, K. E.; Carlton, A. G.; Lim, H. J.; Turpin, B. J.; Seitzinger, S. P., Evidence for oligomer
26 formation in clouds: Reactions of isoprene oxidation products. *Environmental science & technology*
27 **2006**, *40* (16), 4956-4960.
- 28 36. Fang, Y.; Riahi, S.; McDonald, A. T.; Shrestha, M.; Tobias, D. J.; Grassian, V. H., What is the driving
29 force behind the adsorption of hydrophobic molecules on hydrophilic surfaces? *Journal of Physical*
30 *Chemistry Letters* **2019**, *10* (3), 468-473.
- 31 37. Fu, Y.; Zhang, Y.; Zhang, F.; Chen, J.; Zhu, Z.; Yu, X.-Y., Does interfacial photochemistry play a role
32 in the photolysis of pyruvic acid in water? *Atmospheric Environment* **2018**, *191*, 36-45.
- 33 38. Gao, S.; Ng, N. L.; Keyword, M.; Varutbangkul, V.; Bahreini, R.; Nenes, A.; He, J.; Yoo, K. Y.;
34 Beauchamp, J.; Hodyss, R. P., Particle phase acidity and oligomer formation in secondary organic
35 aerosol. *Environmental science & technology* **2004**, *38* (24), 6582-6589.
- 36 39. Kalberer, M.; Paulsen, D.; Sax, M.; Steinbacher, M.; Dommen, J.; Prévôt, A. S.; Fisseha, R.;
37 Weingartner, E.; Frankevich, V.; Zenobi, R., Identification of polymers as major components of
38 atmospheric organic aerosols. *Science* **2004**, *303* (5664), 1659-1662.
- 39 40. Reddy, S. K.; Thiriaux, R.; Rudd, B. A. W.; Lin, L.; Adel, T.; Joutsuka, T.; Geiger, F. M.; Allen, H. C.;
40 Morita, A.; Paesani, F., Bulk contributions modulate the sum-frequency generation spectra of water on
41 model sea-spray aerosols. *Chem* **2018**, *4* (7), 1629-1644.
- 42 41. Tolocka, M. P.; Jang, M.; Ginter, J. M.; Cox, F. J.; Kamens, R. M.; Johnston, M. V., Formation of
43 oligomers in secondary organic aerosol. *Environmental science & technology* **2004**, *38* (5), 1428-1434.
- 44 42. Trueblood, J. V.; Alves, M. R.; Power, D.; Santander, M. V.; Cochran, R. E.; Prather, K. A.;
45 Grassian, V. H., Shedding light on photosensitized reactions within marine-relevant organic thin films.
46 *ACS Earth and Space Chemistry* **2019**, *3* (8), 1614-1623.
- 47 43. Eiseenthal, K., Liquid interfaces probed by second-harmonic and sum-frequency spectroscopy.
48 *Chemical Reviews* **1996**, *96* (4), 1343-1360.
- 49 44. Geissler, P. L., Water interfaces, solvation, and spectroscopy. *Annual Review of Physical*
50 *Chemistry* **2013**, *64*, 317-37.
- 51
52
53
54
55
56
57
58
59
60

- 1
2
3 45. Gordon, B. P.; Moore, F. G.; Scatena, L. F.; Richmond, G. L., On the rise: Experimental and
4 computational vibrational sum frequency spectroscopy studies of pyruvic acid and its surface active
5 oligomer species at the air-water interface. *Journal of Physical Chemistry A* **2019**, *123* (49), 10609-10619.
- 6 46. Jungwirth, P.; Tobias, D. J., Ions at the air/water interface. *The Journal of Physical Chemistry B*
7 **2002**, *106* (25), 6361-6373.
- 8 47. Medders, G. R.; Paesani, F., Dissecting the molecular structure of the air/water interface from
9 quantum simulations of the sum-frequency generation spectrum. *Journal of the American Chemical*
10 *Society* **2016**, *138* (11), 3912-9.
- 11 48. Morita, A.; Hynes, J. T., A theoretical analysis of the sum frequency generation spectrum of the
12 water surface. *Chemical Physics* **2000**, *258* (2-3), 371-390.
- 13 49. Mucha, M.; Frigato, T.; Levering, L. M.; Allen, H. C.; Tobias, D. J.; Dang, L. X.; Jungwirth, P.,
14 Unified molecular picture of the surfaces of aqueous acid, base, and salt solutions. *Journal of Physical*
15 *Chemistry B* **2005**, *109* (16), 7617-23.
- 16 50. Qian, Y.; Deng, G.; Rao, Y., In-situ spectroscopic probing of polarity and molecular configuration
17 at aerosol particle surfaces. *The journal of physical chemistry letters* **2020**.
- 18 51. Richmond, G., Molecular bonding and interactions at aqueous surfaces as probed by vibrational
19 sum frequency spectroscopy. *Chemical Reviews* **2002**, *102* (8), 2693-2724.
- 20 52. Scatena, L.; Brown, M.; Richmond, G., Water at hydrophobic surfaces: Weak hydrogen bonding
21 and strong orientation effects. *Science* **2001**, *292* (5518), 908-912.
- 22 53. Shen, Y. R.; Ostroverkhov, V., Sum-frequency vibrational spectroscopy on water interfaces: Polar
23 orientation of water molecules at interfaces. *Chemical Reviews* **2006**, *106* (4), 1140-1154.
- 24 54. Verreault, D.; Hua, W.; Allen, H. C., From conventional to phase-sensitive vibrational sum
25 frequency generation spectroscopy: Probing water organization at aqueous interfaces. *Journal of*
26 *Physical Chemistry Letters* **2012**, *3* (20), 3012-3028.
- 27 55. Sui, X.; Zhou, Y.; Zhang, F.; Chen, J.; Zhu, Z.; Yu, X.-Y., Deciphering the aqueous chemistry of
28 glyoxal oxidation with hydrogen peroxide using molecular imaging. *Physical Chemistry Chemical Physics*
29 **2017**, *19* (31), 20357-20366.
- 30 56. Zhang, F.; Yu, X.; Chen, J.; Zhu, Z.; Yu, X.-Y., Dark air-liquid interfacial chemistry of glyoxal and
31 hydrogen peroxide. *npj Climate and Atmospheric Science* **2019**, *2* (1), 1-8.
- 32 57. Zhang, F.; Yu, X.; Sui, X.; Chen, J.; Zhu, Z.; Yu, X.-Y., Evolution of aqsoa from the air-liquid
33 interfacial photochemistry of glyoxal and hydroxyl radicals. *Environmental science & technology* **2019**,
34 *53* (17), 10236-10245.
- 35 58. Tervahattu, H.; Juhanaja, J.; Kupiainen, K., Identification of an organic coating on marine aerosol
36 particles by tof-sims. *Journal of Geophysical Research: Atmospheres* **2002**, *107* (D16), ACH 18-1-ACH 18-
37 7.
- 38 59. Tervahattu, H.; Juhanaja, J.; Vaida, V.; Tuck, A.; Niemi, J. V.; Kupiainen, K.; Kulmala, M.;
39 Vehkamäki, H., Fatty acids on continental sulfate aerosol particles. *Journal of Geophysical Research:*
40 *Atmospheres* **2005**, *110* (D6).
- 41 60. Kumar, J. K.; Oliver, J. S., Proximity effects in monolayer films: Kinetic analysis of amide bond
42 formation at the air- water interface using 1h nmr spectroscopy. *Journal of the American Chemical*
43 *Society* **2002**, *124* (38), 11307-11314.
- 44 61. Ciuraru, R.; Fine, L.; Van Pinxteren, M.; D'Anna, B.; Herrmann, H.; George, C., Photosensitized
45 production of functionalized and unsaturated organic compounds at the air-sea interface. *Scientific*
46 *Reports* **2015**, *5*, 12741.
- 47 62. Fu, H.; Ciuraru, R.; Dupart, Y.; Passananti, M.; Tinel, L.; Rossignol, S. p.; Perrier, S.; Donaldson, D.
48 J.; Chen, J.; George, C., Photosensitized production of atmospherically reactive organic compounds at
49 the air/aqueous interface. *Journal of the American Chemical Society* **2015**, *137* (26), 8348-8351.
- 50
51
52
53
54
55
56
57
58
59
60

- 1
2
3 63. Reed Harris, A. E.; Ervens, B.; Shoemaker, R. K.; Kroll, J. A.; Rapf, R. J.; Griffith, E. C.; Monod, A.;
4 Vaida, V., Photochemical kinetics of pyruvic acid in aqueous solution. *Journal of Physical Chemistry A*
5 **2014**, *118* (37), 8505-8516.
- 6 64. Renard, P.; Reed Harris, A. E.; Rapf, R. J.; Ravier, S.; Demelas, C.; Coulomb, B.; Quivet, E.; Vaida,
7 V.; Monod, A., Aqueous phase oligomerization of methyl vinyl ketone by atmospheric radical reactions.
8 *The Journal of Physical Chemistry C* **2014**, *118* (50), 29421-29430.
- 9 65. Shrestha, M.; Luo, M.; Li, Y.; Xiang, B.; Xiong, W.; Grassian, V. H., Let there be light: Stability of
10 palmitic acid monolayers at the air/salt water interface in the presence and absence of simulated solar
11 light and a photosensitizer. *Chemical science* **2018**, *9* (26), 5716-5723.
- 12 66. Vaida, V., Atmospheric radical chemistry revisited. *Science* **2016**, *353* (6300), 650-650.
- 13 67. Andreae, M. O.; Talbot, R. W.; Li, S. M., Atmospheric measurements of pyruvic and formic-acid.
14 *Journal of Geophysical Research-Atmospheres* **1987**, *92* (D6), 6635-6641.
- 15 68. Eger, P. G.; Schuladen, J.; Sobanski, N.; Fischer, H.; Karu, E.; Williams, J.; Riva, M.; Zha, Q.; Ehn,
16 M.; Quéléver, L. L., Pyruvic acid in the boreal forest: Gas-phase mixing ratios and impact on radical
17 chemistry. *Atmospheric Chemistry & Physics* **2020**, *20* (6).
- 18 69. Guzmán, M.; Hoffmann, M.; Colussi, A., Photolysis of pyruvic acid in ice: Possible relevance to co
19 and co2 ice core record anomalies. *Journal of Geophysical Research: Atmospheres* **2007**, *112* (D10).
- 20 70. Shiraiwa, M.; Zuend, A.; Bertram, A. K.; Seinfeld, J. H., Gas-particle partitioning of atmospheric
21 aerosols: Interplay of physical state, non-ideal mixing and morphology. *Physical Chemistry Chemical*
22 *Physics* **2013**, *15* (27), 11441-11453.
- 23 71. Cody, G. D.; Boctor, N. Z.; Filley, T. R.; Hazen, R. M.; Scott, J. H.; Sharma, A.; Yoder, H. S.,
24 Primordial carbonylated iron-sulfur compounds and the synthesis of pyruvate. *Science* **2000**, *289* (5483),
25 1337-1340.
- 26 72. Cooper, G.; Reed, C.; Nguyen, D.; Carter, M.; Wang, Y., Detection and formation scenario of citric
27 acid, pyruvic acid, and other possible metabolism precursors in carbonaceous meteorites. *Proceedings*
28 *of the National Academy of Sciences* **2011**, *108* (34), 14015-14020.
- 29 73. Griffith, E. C.; Shoemaker, R. K.; Vaida, V., Sunlight-initiated chemistry of aqueous pyruvic acid:
30 Building complexity in the origin of life. *Origins of Life and Evolution of Biospheres* **2013**, *43* (4-5), 341-
31 352.
- 32 74. Guzman, M. I.; Martin, S. T., Prebiotic metabolism: Production by mineral
33 photoelectrochemistry of α -ketocarboxylic acids in the reductive tricarboxylic acid cycle. *Astrobiology*
34 **2009**, *9* (9), 833-842.
- 35 75. Pizzarello, S.; Shock, E., The organic composition of carbonaceous meteorites: The evolutionary
36 story ahead of biochemistry. *Cold Spring Harbor perspectives in biology* **2010**, *2* (3), a002105.
- 37 76. Shapiro, R., Small molecule interactions were central to the origin of life. *Quarterly Review of*
38 *Biology* **2006**, *81* (2), 105-125.
- 39 77. Berges, M. G.; Warneck, P., Product quantum yields for the 350 nm photodecomposition of
40 pyruvic acid in air. *Berichte der Bunsengesellschaft für physikalische Chemie* **1992**, *96* (3), 413-416.
- 41 78. Grosjean, D., Atmospheric reactions of pyruvic acid. *Atmospheric Environment (1967)* **1983**, *17*
42 (11), 2379-2382.
- 43 79. Harris, A. E. R.; Cazaunau, M.; Gratien, A.; Pangu, E.; Doussin, J. F.; Vaida, V., Atmospheric
44 simulation chamber studies of the gas-phase photolysis of pyruvic acid. *Journal of Physical Chemistry A*
45 **2017**, *121* (44), 8348-8358.
- 46 80. Leermakers, P. A.; Vesley, G. F., The photochemistry of α -keto acids and α -keto esters. I.
47 Photolysis of pyruvic acid and benzoylformic acid. *Journal of the American Chemical Society* **1963**, *85*
48 (23), 3776-3779.
- 49 81. Mellouki, A.; Mu, Y., On the atmospheric degradation of pyruvic acid in the gas phase. *Journal of*
50 *Photochemistry and Photobiology A: Chemistry* **2003**, *157* (2-3), 295-300.
- 51
52
53
54
55
56
57
58
59
60

- 1
2
3 82. Reed Harris, A. E.; Doussin, J. F.; Carpenter, B. K.; Vaida, V., Gas-phase photolysis of pyruvic acid:
4 The effect of pressure on reaction rates and products. *Journal of Physical Chemistry A* **2016**, *120* (51),
5 10123-10133.
6
7 83. Sutradhar, S.; Samanta, B. R.; Fernando, R.; Reisler, H., Spectroscopy and two-photon
8 dissociation of jet-cooled pyruvic acid. *The Journal of Physical Chemistry A* **2019**, *123* (28), 5906-5917.
9
10 84. Takahashi, K.; Plath, K. L.; Skodje, R. T.; Vaida, V., Dynamics of vibrational overtone excited
11 pyruvic acid in the gas phase: Line broadening through hydrogen-atom chattering. *The Journal of*
12 *Physical Chemistry A* **2008**, *112* (32), 7321-7331.
13
14 85. Vesley, G. F.; Leermakers, P. A., The photochemistry of α -keto acids and α -keto esters. lli.
15 Photolysis of pyruvic acid in the vapor phase. *The Journal of Physical Chemistry* **1964**, *68* (8), 2364-2366.
16
17 86. Yamamoto, S.; Back, R. A., The photolysis and thermal-decomposition of pyruvic-acid in the gas-
18 phase. *Canadian Journal of Chemistry-Revue Canadienne De Chimie* **1985**, *63* (2), 549-554.
19
20 87. Church, J. R.; Vaida, V.; Skodje, R. T., Gas-phase reaction kinetics of pyruvic acid with oh radicals:
21 The role of tunneling, complex formation, and conformational structure. *The Journal of Physical*
22 *chemistry. A* **2020**, *124* (5), 790-800.
23
24 88. Chang, X.-P.; Fang, Q.; Cui, G., Mechanistic photodecarboxylation of pyruvic acid: Excited-state
25 proton transfer and three-state intersection. *The Journal of chemical physics* **2014**, *141* (15), 154311.
26
27 89. da Silva, G., Decomposition of pyruvic acid on the ground-state potential energy surface. *The*
28 *Journal of Physical Chemistry A* **2016**, *120* (2), 276-283.
29
30 90. Eugene, A. J.; Guzman, M. I., Reactivity of ketyl and acetyl radicals from direct solar actinic
31 photolysis of aqueous pyruvic acid. *The Journal of Physical Chemistry A* **2017**, *121* (15), 2924-2935.
32
33 91. Eugene, A. J.; Guzman, M. I., The effects of reactant concentration and air flow rate in the
34 consumption of dissolved o-2 during the photochemistry of aqueous pyruvic acid. *Molecules* **2019**, *24*
35 (6).
36
37 92. Griffith, E. C.; Carpenter, B. K.; Shoemaker, R. K.; Vaida, V., Photochemistry of aqueous pyruvic
38 acid. *Proceedings of the National Academy of Sciences of the United States of America* **2013**, *110* (29),
39 11714-11719.
40
41 93. Griffith, E. C.; Carpenter, B. K.; Shoemaker, R. K.; Vaida, V., Reply to eugene et al.:
42 Photochemistry of aqueous pyruvic acid. *Proceedings of the National Academy of Sciences of the United*
43 *States of America* **2013**, *110* (46), E4276-E4276.
44
45 94. Griffith, E. C.; Rapf, R. J.; Shoemaker, R. K.; Carpenter, B. K.; Vaida, V., Photoinitiated synthesis of
46 self-assembled vesicles. *Journal of the American Chemical Society* **2014**, *136* (10), 3784-3787.
47
48 95. Guzman, M. I.; Colussi, A. J.; Hoffmann, M. R., Photoinduced oligomerization of aqueous pyruvic
49 acid. *Journal of Physical Chemistry A* **2006**, *110* (10), 3619-3626.
50
51 96. Larsen, M. C.; Vaida, V., Near infrared photochemistry of pyruvic acid in aqueous solution. *The*
52 *Journal of Physical Chemistry A* **2012**, *116* (24), 5840-5846.
53
54 97. Leermakers, P.; Vesley, G., Photolysis of pyruvic acid in solution. *Journal of Organic Chemistry*
55 **1963**, *28* (4), 1160-&.
56
57 98. Mekic, M.; Brigante, M.; Vione, D.; Gligorovski, S., Exploring the ionic strength effects on the
58 photochemical degradation of pyruvic acid in atmospheric deliquescent aerosol particles. *Atmospheric*
59 *Environment* **2018**, *185*, 237-242.
60
99. Rapf, R. J.; Perkins, R. J.; Carpenter, B. K.; Vaida, V., Mechanistic description of photochemical
oligomer formation from aqueous pyruvic acid. *Journal of Physical Chemistry A* **2017**, *121* (22), 4272-
4282.
100. Davidson, R. S.; Goodwin, D.; De Violet, P. F., The mechanism of the photo-induced
decarboxylation of pyruvic acid in solution. *Chemical Physics Letters* **1981**, *78* (3), 471-474.
101. Guzman, M.; Colussi, A.; Hoffmann, M., Photoinduced oligomerization of aqueous pyruvic acid.
The Journal of Physical Chemistry A **2006**, *110* (10), 3619-3626.

102. Rapf, R. J.; Dooley, M. R.; Kappes, K.; Perkins, R. J.; Vaida, V., Ph dependence of the aqueous photochemistry of alpha-keto acids. *Journal of Physical Chemistry A* **2017**, *121* (44), 8368-8379.
103. Rincón, A. G.; Guzmán, M. I.; Hoffmann, M. R.; Colussi, A., Optical absorptivity versus molecular composition of model organic aerosol matter. *The Journal of Physical Chemistry A* **2009**, *113* (39), 10512-10520.
104. Wang, J.; Doussin, J. F.; Perrier, S.; Perraudin, E.; Katrib, Y.; Pangui, E.; Picquet-Varrault, B., Design of a new multi-phase experimental simulation chamber for atmospheric photosmog, aerosol and cloud chemistry research. *Atmospheric Measurement Techniques* **2011**, *4* (11), 2465-2494.
105. Perkins, R. J.; Shoemaker, R. K.; Carpenter, B. K.; Vaida, V., Chemical equilibria and kinetics in aqueous solutions of zymonic acid. *Journal of Physical Chemistry A* **2016**, *120* (51), 10096-10107.
106. Eliason, T. L.; Gilman, J. B.; Vaida, V., Oxidation of organic films relevant to atmospheric aerosols. *Atmospheric Environment* **2004**, *38* (9), 1367-1378.
107. Gilman, J. B.; Eliason, T. L.; Fast, A.; Vaida, V., Selectivity and stability of organic films at the air-aqueous interface. *Journal of Colloid and Interface Science* **2004**, *280* (1), 234-243.
108. Griffith, E. C.; Adams, E. M.; Allen, H. C.; Vaida, V., Hydrophobic collapse of a stearic acid film by adsorbed l-phenylalanine at the air-water interface. *Journal of Physical Chemistry B* **2012**, *116* (27), 7849-7857.
109. Griffith, E. C.; Guizado, T. R. C.; Pimentel, A. S.; Tyndall, G. S.; Vaida, V., Oxidized aromatic-aliphatic mixed films at the air-aqueous solution interface. *The Journal of Physical Chemistry C* **2013**, *117* (43), 22341-22350.
110. Griffith, E. C.; Perkins, R. J.; Telesford, D. M.; Adams, E. M.; Cwiklik, L.; Allen, H. C.; Roeselova, M.; Vaida, V., Interaction of l-phenylalanine with a phospholipid monolayer at the water-air interface. *Journal of Physical Chemistry B* **2015**, *119* (29), 9038-9048.
111. Perkins, R. J.; Kukharchuk, A.; Delcroix, P.; Shoemaker, R. K.; Roeselova, M.; Cwiklik, L.; Vaida, V., The partitioning of small aromatic molecules to air-water and phospholipid interfaces mediated by non-hydrophobic interactions. *Journal of Physical Chemistry B* **2016**, *120* (30), 7408-7422.
112. Rapf, R.; Griffith, E.; Vaida, V., Sunlight-driven synthesis and self-assembly of a model amphiphile at the air-water interface. *Abstracts of Papers of the American Chemical Society* **2015**, 249.
113. Rapf, R. J.; Perkins, R. J.; Yang, H. S.; Miyake, G.; Carpenter, B. K.; Vaida, V., Photochemical synthesis of oligomeric amphiphiles from alkyl oxoacids in aqueous environments. *Journal of the American Chemical Society* **2017**, *139* (20), 6946-6959.
114. Bregonzio-Rozier, L.; Siekmann, F.; Giorio, C.; Pangui, E.; Morales, S. B.; Temime-Roussel, B.; Gratien, A.; Michoud, V.; Ravier, S.; Cazaunau, M.; Tapparo, A.; Monod, A.; Doussin, J. F., Gaseous products and secondary organic aerosol formation during long term oxidation of isoprene and methacrolein. *Atmospheric Chemistry and Physics* **2015**, *15* (6), 2953-2968.
115. Kramer, Z. C.; Takahashi, K.; Vaida, V.; Skodje, R. T., Will water act as a photocatalyst for cluster phase chemical reactions? Vibrational overtone-induced dehydration reaction of methanediol. *The Journal of Chemical Physics* **2012**, *136* (16), 164302.
116. Maroń, M. K.; Takahashi, K.; Shoemaker, R. K.; Vaida, V., Hydration of pyruvic acid to its geminal-diol, 2, 2-dihydroxypropanoic acid, in a water-restricted environment. *Chemical Physics Letters* **2011**, *513* (4-6), 184-190.
117. Donaldson, D. J.; Tervahattu, H.; Tuck, A. F.; Vaida, V., Organic aerosols and the origin of life: An hypothesis. *Origins of Life and Evolution of Biospheres* **2004**, *34* (1-2), 57-67.
118. Donaldson, D. J.; Tuck, A. F.; Vaida, V., The asymmetry of organic aerosol fission and prebiotic chemistry. *Origins of Life and Evolution of the Biosphere* **2002**, *32* (3), 237-245.
119. Vaida, V., Ocean sea spray, clouds, and climate. *Acs Central Science* **2015**, *1* (3), 112-114.
120. Vaida, V., Prebiotic phosphorylation enabled by microdroplets. *Proceedings of the National Academy of Sciences of the United States of America* **2017**, *114* (47), 12359-12361.

- 1
2
3 121. Sui, X.; Zhou, Y.; Zhang, F.; Zhang, Y.; Chen, J.; Zhu, Z.; Yu, X. Y., Tof-sims characterization of
4 glyoxal surface oxidation products by hydrogen peroxide: A comparison between dry and liquid samples.
5 *Surface and Interface Analysis* **2018**, *50* (10), 927-938.
6
7 122. Karp, G., *Cell and molecular biology: Concepts and experiments*. John Wiley & Sons: 2009.
8 123. Schwarz, H. A.; Dodson, R. W., Equilibrium between hydroxyl radicals and thallium(ii) and the
9 oxidation potential of oh(aq). *Journal of Physical Chemistry* **1984**, *88* (16), 3643-3647.
10 124. Agmon, N.; Bakker, H. J.; Campen, R. K.; Henchman, R. H.; Pohl, P.; Roke, S.; Thamer, M.;
11 Hassanali, A., Protons and hydroxide ions in aqueous systems. *Chemical Reviews* **2016**, *116* (13), 7642-
12 72.
13 125. Buch, V.; Milet, A.; Vacha, R.; Jungwirth, P.; Devlin, J. P., Water surface is acidic. *Proceedings of*
14 *the National Academy of Sciences of the United States of America* **2007**, *104* (18), 7342-7347.
15 126. Tse, Y. L.; Chen, C.; Lindberg, G. E.; Kumar, R.; Voth, G. A., Propensity of hydrated excess protons
16 and hydroxide anions for the air-water interface. *Journal of the American Chemical Society* **2015**, *137*
17 (39), 12610-6.
18 127. Kathmann, S. M.; Kuo, I. F. W.; Mundy, C. J., Electronic effects on the surface potential at the
19 vapor-liquid interface of water (vol 130, 16556, 2008). *Journal of the American Chemical Society* **2009**,
20 *131* (47), 17522-17522.
21 128. Paluch, M., Surface potential at the water-air interface. *Annales Universitatis Mariae Curie-*
22 *Sklodowska, sectio AA-Chemia* **2016**, *70* (2), 1.
23
24
25
26

TOC Graphic

